rubicin (17,18), camptothecin (19), paclitaxel (20), and cisplatin (21).

In our previous study, ATRA was successfully incorporated in poly(ethylene glycol)-poly(aspartate ester) (PEG-P(Asp)) block copolymer micelles in which 75% of the aspartic acid residues were esterified benzyl groups in order to increase the hydrophobicity of the inner core (22). Because ATRA is a hydrophobic drug, the interaction between ATRA and the hydrophobic inner core play a very important role in the stable incorporation. The ATRA polymeric micelles were effective in increasing the blood retention and lowering hepatic clearance compared with free ATRA and ATRA incorporated in liposomes and suggested the potential use of this system for the design of ATRA carriers in the treatment of solid tumors.

In the present study, the distribution and antitumor efficacy of ATRA incorporated in polymeric micelles was examined in mice bearing CT26 solid tumors. The distribution characteristics of ATRA delivered by polymeric micelles showed a prolonged blood retention and enhanced accumulation of ATRA at the tumor site. Finally, we evaluated the efficiency of ATRA incorporated in polymeric micelles for the treatment of solid tumors by measuring the tumor volume and survival of the mice.

MATERIALS AND METHODS

Chemical

ATRA was purchased from Wako Pure Chemicals Industry, Ltd. (Osaka, Japan). Clear-Sol I was obtained from Nacalai Tesque, Inc. (Kyoto, Japan), and Soluene 350 was purchased from Packard Co., Inc. (Groningen, The Netherlands). RPMI1640 medium was obtained from Nissui Pharmaceutical Co., Ltd. (Tokyo, Japan). Fetal bovine serum (FBS) was purchased from Biowhittaker (Walkersville, MD, USA). HCO-60 was obtained from Nikko Chemical Co. Ltd. (Japan). [^{3}H]ATRA was purchased from NEN Life Science Products, Inc. (Boston, USA). All other chemicals were of the highest purity available.

Synthesis of Block Copolymer

PEG-P(Asp) block copolymer was obtained by alkaline hydrolysis of poly(ethylene glycol)-poly(β-benzyl-L-aspatate) (PEG-PBLA) as reported previously (23). Briefly, the molecular weight of the poly(ethylene glycol) (PEG) chain was 5,000 and the average number of aspartic acid units was 27. Approximately 69% of the aspartic acid residues in the poly(aspartic acid) chain were converted to the β-amide form by alkaline hydrolysis during the synthesis of this block copolymer. A hydrophobic benzyl group was bound to 69% of the poly(aspartic acid) residues by an ester-forming reaction between benzyl bromide and PEG-P(Asp) as reported previously (24). Briefly, PEG-P(Asp) block copolymer was dissolved in *N,N*-dimethylformamide (DMF) and added to benzyl bromide along with a catalyst, 1, 8-diazabicyclo[5,4,0]7-undecene (DBU). The reaction mixture was stirred at 50°C for 15.5 h. Polymers were obtained by precipitation in an excess of diethyl ether and collected by filtration. The dried polymer was dissolved in dimethyl sulfoxide (DMSO), then 6 N HCl was added, followed by dialysis against distilled water and, finally, freeze-drying.

For determination of the polymer composition, such as the number of Asp units and the benzyl ester content, ^{1}H-NMR measurements were carried out on a 1% solution in 6D-DMSO containing 3% trifluoroacetic acid using a Varian Unity Inova NMR spectrometer at 400 MHz.

Incorporation of ATRA into Polymeric Micelles

Incorporation of ATRA into polymeric micelles was carried out by an evaporation method as previously described (22). Briefly, ATRA 1 mg and polymer 10 mg were dissolved in chloroform. After vacuum drying and desiccation, 3 ml of phosphate buffered saline (PBS) pH7.4 was added for hydration for 30 min at 25°C. The preparation was placed in the probe sonicator (200 W) for 3 min at 60°C. The obtained preparation was centrifuged at 1,500×*g* for 10 min before the supernatant was passed through a 0.450-μm filter. The maximum concentration of ATRA in the polymeric micelle preparation was about 0.066 mg/ml that quantified by the UV absorption at 340 nm after dissolving the preparation in a mixture of dimethylsulfoxide (DMSO) and water (DMSO:water=9:1 by volume). After the preparation was filtered, the concentration of ATRA in filtered preparation was adjusted to 0.060 mg/ml for *in vivo* experiments based on its UV absorption. The particle size of the polymeric micelles was measured by Zetasizer Nano Series instrument (Malvern Instruments, Ltd., Worcestershire, UK). To prepare [^{3}H]ATRA-labeled polymeric micelles, a trace amount of [^{3}H]ATRA (50 μCi) was dissolved in chloroform with ATRA and polymer and then treated exactly as described above. The filtered ATRA was adjusted to a concentration of 0.06 mg/ml based on the measured radioactivity.

Solubility of ATRA

The solubility of ATRA in serum was determined by mixing the excess amount of ATRA in serum and stirred overnight at 37°C. The undissolved ATRA was separated from the solution by filtration through 0.450-μm filter. The amount of ATRA dissolved in serum was determined by spectrophotometer at 340 nm (UV-visible Spectrophotometer, Shimazu Co., Ltd., Kyoto, Japan). The solubility of ATRA in serum was 1.426±0.009 mg/ml at 37°C (n=3).

In Vitro Cytotoxicity Experiment

3-(4,5-Dimethyl-2-thiazolyl)-2,5-diphenyl-2*H* tetrazolium bromide (MTT) assay was performed by the method described previously (10). The CT-26, mouse colon adenocarcinoma cells, was plated on a 96-well cluster dish at a density of 1×10^4 cells/0.28 cm^2. Twenty-four hours later, the medium containing various concentrations of unloaded polymeric micelles was added to the plates. After 48 h of incubation, the medium was removed and 5 mg/ml MTT solution was added to each well. Cells were incubated for 4 h at 37°C in 5% CO_2 and then 10% sodium dodecyl sulfate (SDS) solution was added followed by incubation overnight to dissolve formazan crystals. The absorbance was measured at wavelengths of 570 nm in a microplate photometer (Bio-

Rad Model 550, Bio-Rad Laboratories, Inc., Hercules, CA, USA).

In Vivo Distribution Experiment

The *in Vivo* distribution study was performed by the method described previously (25). Briefly, five-week-old male ddY mice (23–25 g) were obtained from the Shizuoka Agricultural Cooperative Association for Laboratory Animals (Shizuoka, Japan). [^{3}H]ATRA dispersed in serum or incorporated in polymeric micelles was injected into the tail vein of the mice. At each collection time point, blood was collected from the vena cava under anesthesia, and the mice were killed at the end of the experiment. Ten microliters of blood were incubated with 0.7 ml Soluene 350 overnight at 45°C. Following digestion, 0.2 ml isopropanol, 0.2 ml 30% hydrogen peroxide, 0.1 ml 5N HCl, and 5.0 ml Clear-Sol I were added in this order. The samples were stored overnight and the radioactivity was measured using a liquid scintillation counter (LSA-500, Beckman, Tokyo, Japan).

Tumor Bearing Mouse Model

Four-week-old male CDF1 mice (20–23 g) were purchased from the Shizuoka Agricultural Cooperative Association for Laboratory Animals. CT-26, mouse colon adenocarcinoma cells, were routinely grown in RPMI1640 medium supplemented with 10% FBS, 100 IU/ml penicillin, 100 μg/ml streptomycin, and 2 mM L-glutamine (all from Invitrogen Co., Carlsbad, CA, USA) in 5% CO_2 humidified air at 37°C. The cells were harvested from 2-day-old subconfluent cultures by trypsin and the cell concentration was adjusted to 10^6 cells/ml by Hank's balance salt solution (HBSS). Then, 0.1 ml of the cell suspension was inoculated subcutaneously in the lower back of each CDF1 mouse. A solid tumor was observed within 7 days after tumor inoculation.

Tissue Distribution in Tumor-Bearing Mice

The blood concentration, tissue distribution and tumor accumulation of [^{3}H]ATRA was examined in tumor-bearing mice on day 14 post-inoculation. After injection of [^{3}H]ATRA dispersed in serum or [^{3}H]ATRA polymeric micelles into the tail vein of the mice, blood, tumor and other tissues were collected and the radioactivity was determined as previously described in the *in vivo* distribution experiment.

Anti-Tumor Efficacy in Tumor-Bearing Mice

The anti-tumor efficacy of ATRA was evaluated in CDF1 mice bearing CT26 cells. We and other group demonstrated that intravenous administration of ATRA incorporated in cationic liposome, O/W emulsion, sterylglucoside liposome at dose of ATRA 0.585 or 0.600 mg/kg exhibited anti-tumor in mice model (11,12,26). Therefore, ATRA dispersed in 5% HCO-60 solution or ATRA incorporated in polymeric micelles were repeatedly injected through the tail vein at an ATRA dose of 0.600 mg/kg/day every other day from day 3 to 11 (5 doses administered) after tumor inoculation (seven mice per group). In the control group, saline (10 ml/kg/day) was administered instead of ATRA. The survival of the mice was recorded every day up to 60 days after tumor inoculation. At the same time, tumor volume and body weight were measured for individual animals as long as more than three mice survived. The tumor volume was determined by measuring the tumor diameter with calipers and calculated as follows:

$$\text{Volume} = \pi/6 \times LW^2$$

Where L is the long diameter and W is the short diameter

Statistical Analysis

Statistical comparisons were performed using Student's t test for two groups. Statistical analysis of tumor volume and survival curves was carried out using Dunnett's test and the log-rank test respectively. $P<0.05$ was considered significant.

RESULTS

Characteristics of ATRA Incorporated in Polymeric Micelles

The block copolymer was successfully synthesized from PEG-P(Asp), and about 69% of the aspartic residues were esterified with benzyl groups as reported previously (23). ATRA was incorporated into the polymeric micelles by the evaporation method, and yielded a clear solution after being passed through 0.450 μm filter. The mean particle size (volume) of the micelles after incorporation of ATRA was 36.3±0.624 (73.7±2.54%) and 290±51.9 (25.6±3.50%) (n=3), respectively. The percentage recovery of ATRA in the polymeric micelle solution detected by UV absorption at 340 nm was 14.0±2.0% (n=3) when compared with the initial amount of ATRA. As previously reported the incorporation ratio of ATRA in polymeric micelles was 96.4±0.17% suggesting ATRA almost completely incorporated in micelles (22). The particle size and concentration of ATRA in the polymeric micelle solution remained constant for at least 1 month when stored at 4°C and protected from light under nitrogen gas.

Cytotoxic Effect of Polymeric Micelles

The cytotoxicity of polymeric micelles was evaluated in CT-26 cells and no significant cytotoxicity was observed at the concentration of 2–40 μg/ml of polymeric micelles, suggesting polymeric micelles itself is low cytotoxic (data not shown).

Distribution Characteristics of [^{3}H]ATRA in Mice

Figure 1 shows the blood concentration profiles of [^{3}H]ATRA dispersed in serum (representing the inherent distribution of ATRA) and [^{3}H]ATRA incorporated in polymeric micelles after intravenous injection into mice. The blood concentration of [^{3}H]ATRA in serum was significantly lower than that of [^{3}H]ATRA in polymeric micelles over 4 h suggesting that polymeric micelles with benzyl groups can enhance the blood retention of ATRA by their encapsulation efficacy.

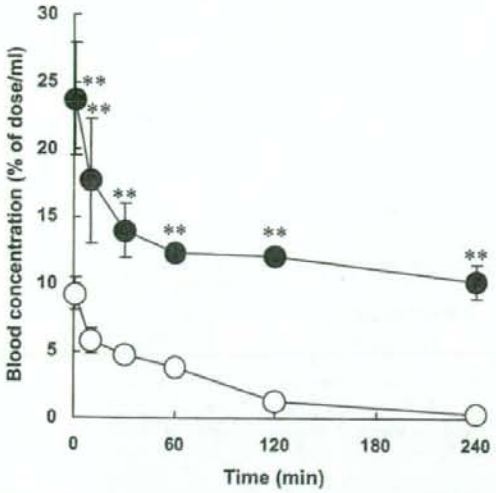

Fig. 1. Blood concentration of [^{3}H]ATRA (*open circle*) and [^{3}H]ATRA incorporated in polymeric micelles (*filled circle*) following intravenous administration to normal mice. Mice were intravenously administered with [^{3}H]ATRA dispersed in serum or [^{3}H]ATRA incorporated in polymeric micelles at 0.600 mg/kg dose of ATRA. At indicated time point, blood was collected and level of radioactivity was measured. Each value represents the mean ± SD of three experiments. Statistically significant differences compared with [^{3}H]ATRA (*double asterisk*, $P<0.01$).

Distribution of [^{3}H]ATRA in Tumor-Bearing Mice

The blood concentration and tumor accumulation of [^{3}H]ATRA dispersed in serum or [^{3}H]ATRA incorporated in polymeric micelles was evaluated in mice bearing CT26 solid tumors. The distribution of [^{3}H]ATRA was determined between 4 and 48 h after a single intravenous injection of 0.600 mg/kg ATRA. The blood concentration of ATRA in polymeric micelles was higher than that of ATRA dispersed in serum at every time point. Following a single injection of ATRA polymeric micelles, the ATRA level was prolonged to almost 48 h while ATRA dispersed in serum was rapidly eliminated and hardly any remained 24 h after administration (Fig. 2a). This sustained blood concentration of ATRA produced by polymeric micelles resulted in a higher accumulation of ATRA in the tumor tissue compared with ATRA dispersed in serum (Fig. 2b). Moreover, the liver accumulation of ATRA delivered by polymeric micelles was

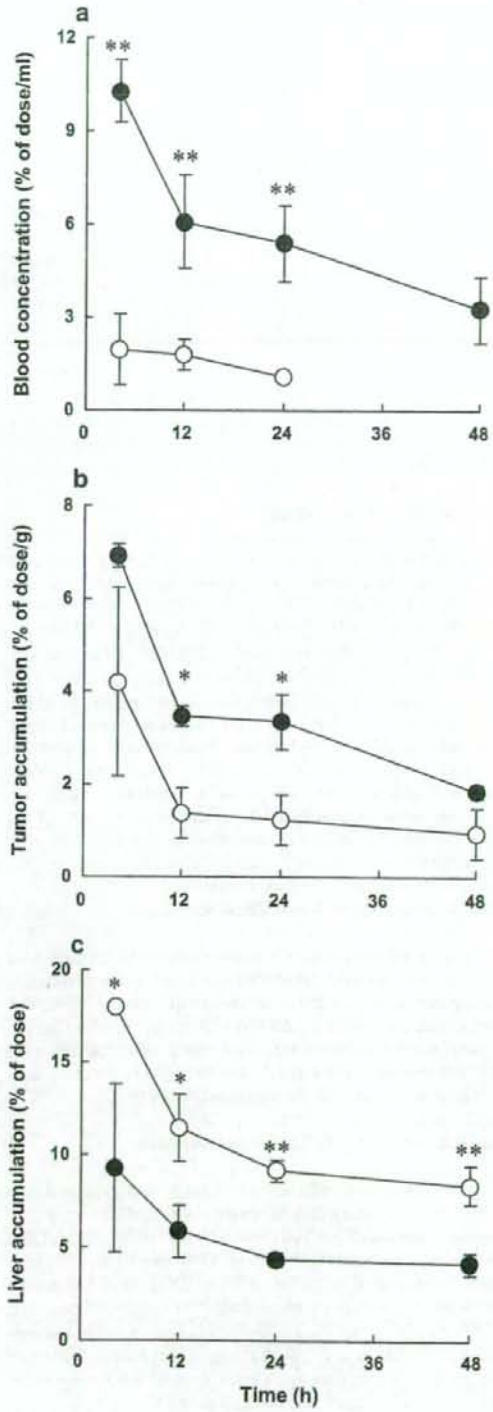

Fig. 2. Blood concentration (**a**), tumor accumulation (**b**), and liver accumulation (**c**) of [^{3}H]ATRA (*open circle*) and [^{3}H]ATRA incorporated in polymeric micelles (*filled circle*) following intravenous administration to tumor-bearing mice. Mice were intravenously administered with [^{3}H]ATRA dispersed in serum or [^{3}H]ATRA incorporated in polymeric micelles at 0.600 mg/kg dose of ATRA. At indicated time point, blood, tumor, and liver were collected and their radioactivity levels were measured. Each value represents the mean±SD of three experiments. Statistically significant differences compared with [^{3}H]ATRA (*double asterisk*, $P<0.01$; *single asterisk*, $P<0.05$).

lower than that of ATRA dispersed in serum (Fig. 2c) suggesting that polymeric micelles could reduce uptake by the liver, lead to retention in the blood and accumulate in the liver tissue. The accumulations of ATRA in lung, spleen, and kidney were very low and almost below the limit of detection within 4 h of injection (data not shown).

Anti-Tumor Effect of ATRA Incorporated in Polymeric Micelles in Tumor-Bearing Mice

The anti-tumor effect of ATRA was evaluated in mice bearing CT26 solid tumors by intravenous administration of saline (control), ATRA in HCO-60 micelles and ATRA in polymeric micelles at an ATRA dosage of 0.600 mg/kg/day or injection of 10 ml/kg/day every other day from day 3 to day 11. The body weight of mice ranged from 19 to 26 g regardless of the treatment group (data not shown). The results demonstrate that only ATRA in polymeric micelles delayed the growth of tumor lesions when compared with the controls treated with saline, while ATRA in HCO-60 micelles with the same administered dose of ATRA did not have any effect on tumor growth (Fig. 3). It was found that the tumor volume correlated with the survival of the mice and the mice died when the tumor reached around 4 cm^3. Following treatment with ATRA polymeric micelles, the survival time of tumor bearing mice was increased (median survival time=50 days) when compared with the control mice treated with saline (median survival time=29 days) and ATRA in HCO-60 micelles (median survival time=37 days; Fig. 4).

DISCUSSION

Polymeric micelles have attracted particular interest as a carrier for anti-tumor drugs, including ATRA, by enhancing drug retention in tumors by an EPR effect. Recently, Zuccari *et al.* (27) developed ATRA polymeric micelles by forming a complex of between ATRA and the modified polyvinylalcohol (PVA) substituted with oleylamine and showed enhanced

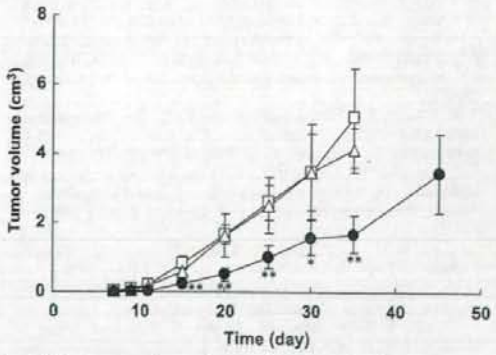

Fig. 3. The tumor volume of tumor-bearing mice after intravenous administration of saline (*open square*), ATRA in HCO-60 micelles (*open triangle*), and ATRA incorporated in polymeric micelles (*filled circle*) at 3, 5, 7, 9, and 11 days (total five doses administered) after tumor inoculation. Each value represents the mean±SD of seven mice. Statistically significant differences compared with the administration of saline (*double asterisk*, $P<0.01$; *single asterisk*, $P<0.05$).

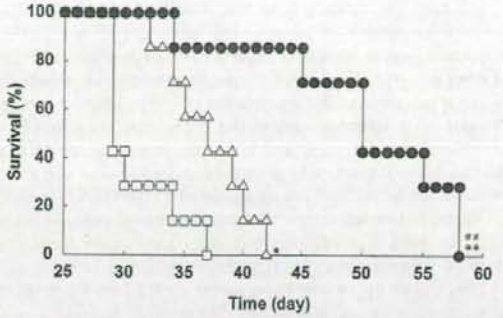

Fig. 4. Survival time of tumor-bearing mice after intravenous administration of saline (*open square*), ATRA in HCO-60 micelles (*open triangle*), and ATRA incorporated in polymeric micelles (*filled circle*) at 3, 5, 7, 9, and 11 days (total five doses administered) after tumor inoculation. Survival of mice was observed daily for 58 days and the percentage survival of each group (seven mice per group) is represented. Statistically significant differences compared with the administration of saline (*double asterisk*, $P<0.01$; *single asterisk*, $P<0.05$) and the administration of ATRA in HCO-60 micelles (*double pound sign*, $P<0.01$).

cytotoxicity of the drug towards neuroblastoma cells compared with pure ATRA. Moreover, Jeong *et al.* developed a poly(ε-caprolactone)/poly(ethylene glycol) diblock copolymer for ATRA incorporation. They examined the ATRA incorporation into polymeric micelles and ATRA release and demonstrated that the ATRA incorporation efficacy is increased by the molecular weight of hydrophobic poly(ε-caprolactone) in the poly(ε-caprolactone)/poly(ethylene glycol) diblock copolymer (28). Although these studies showed the advantages of polymeric micelles as ATRA carriers, the *in vitro* studies were not enough to provide any information about their therapeutic effectiveness. In this regard, the present study was performed to evaluate the *in vivo* efficiency of ATRA incorporated in polymeric micelles for anticancer therapy.

Since ATRA is a highly lipophilic drug (log PC_{oct}=6.6) (29), it was stably incorporated in the lipophilic inner core of the polymeric micelles and was protected from elimination by a hydrophilic outer shell. Moreover, the particle size of the prepared ATRA polymeric micelles around 160 nm provides a system to reduce elimination by the RES, prolong the retention in blood vessels, and allow passage through the leaky vasculature into the interstitial space of the tumor tissue. Therefore, the anticancer activity of ATRA would be enhanced by the incorporation in polymeric micelles.

The biodistribution of the prepared [^{3}H]ATRA polymeric micelles and [^{3}H]ATRA dispersed in serum (30,31) which represents the inherent distribution of ATRA after intravenous administration into normal mice was examined in order to compare the distribution characteristics of ATRA. As shown in Fig. 1, [^{3}H]ATRA dispersed in serum was rapidly eliminated from the blood. In contrast, [^{3}H]ATRA was significantly retained in the blood circulation when ATRA was incorporated in polymeric micelles. These results lead us to believe that when ATRA was incorporated in polymeric micelles with 69% benzyl ester groups this resulted in sustained blood concentrations of ATRA.

Since the retention in the blood circulation would benefit the passive diffusion of the molecules allowing them to accumulate in the tumor tissue by the EPR effect (16), the distribution of [^{3}H]ATRA was also evaluated in mice bearing CT26 solid tumors. The distribution of [^{3}H]ATRA in tumor-bearing mice corresponded to that in normal mice in which the blood concentration and tumor accumulation of ATRA after administration with polymeric micelles was sustained whereas the intratumor concentration of [^{3}H]ATRA dispersed in serum fell rapidly in parallel with the blood concentration (Fig. 2a and b). In addition, the lower liver accumulation of ATRA polymeric micelles (Fig. 2c) suggested a reduction of ATRA taken up by the hepatocytes or RES that benefited the retention of ATRA in the blood. Our results in prolonging the blood concentration and enhancing tumor accumulation suggested that the EPR effect plays a role in this tumor accumulation.

To investigate whether polymeric micelle-enhanced ATRA accumulated in solid tumors can improve the anticancer activity of ATRA, the therapeutic efficiency of ATRA incorporated in polymeric micelles was evaluated in tumor-bearing mice. The delayed tumor growth produced by ATRA incorporated in polymeric micelles (Fig. 3) demonstrated that ATRA incorporated in polymeric micelles exhibited superior activity against tumors compared with the administration of saline or ATRA dispersed in HCO-60 micelles. The increased survival time of tumor-bearing mice treated with ATRA in polymeric micelles compared with other treatment groups (Fig. 4) confirmed the potential therapeutic efficacy of ATRA incorporated in polymeric micelles. Altogether, these results confirmed the therapeutic efficiency of the micellar structure of PEG-P(Asp) block copolymer with 69% benzyl ester groups as an effective delivery system of ATRA to solid tumors to exert its anti-cancer activity.

One of the most interesting features of polymeric micelles is the small particle size that blocks uptake by the RES and extravasation in the tumor tissue. However, the particle size of the partial polymeric micelles in the present study was larger than previously reported (22). This may be due to the increased concentration of the prepared ATRA polymeric micelles (from 1.667 to 3.333 mg/ml) that might induce temporary aggregation of the particles during storage. However, they were small enough to escape RES scavenging and enhanced the permeability and retention at the solid tumor site since their particle size remained below 200 nm (32).

ATRA has been widely used as a chemopreventive agent, which exerts strong anti-tumor activity by suppressing tumor growth (33,34). However, like many other anticancer drugs, sophisticated delivery and targeting is required for successful *in vivo* application. Apart from the benefit with regard to the EPR effect, ATRA polymeric micelles may be able to improve the outcome of APL disease since the high plasma concentration would alleviate the progressive decline in the plasma drug concentration after prolonged oral ATRA administration. Although further study is required, ATRA incorporated in polymeric micelles could be useful for cancer differentiation therapy, including the treatment of APL in the future.

In conclusion, we have examined the biodistribution characteristics of ATRA incorporated in polymeric micelles composed of PEG-P(Asp) with 69% esterification after intravenous administration. We have demonstrated that polymeric micelles prolonged the blood retention of ATRA, produced passive accumulation in the tumor site and resulted in superior therapeutic benefits of ATRA in mice with solid CT26 tumors.

ACKNOWLEDGMENTS

This work was supported in part by Grants-in-Aid for Scientific Research and the Program for Promoting the Establishment of Strategic Research Centers, Special Coordination Funds for Promoting Science and Technology from the Ministry of Education, Culture, Sports, Science, and Technology of Japan, and by Health and Labour Sciences Research Grants for Research on Advanced Medical Technology from the Ministry of Health, Labour and Welfare of Japan.

REFERENCES

1. S. Y. Sun, and R. Lotan. Retinoids and their receptors in cancer development and chemoprevention. *Crit. Rev. Oncol. Hematol.* **41**:41–55 (2002).
2. T. Otsuki, H. Sakaguchi, T. Hatayama, P. Wu, A.Takata, and F. Hyodoh. Effects of all-trans retinoic acid (ATRA) on human myeloma cells. *Leuk. Lymphoma.* **44**:1651–1656 (2003).
3. F. Arce, O. Gatjens-Boniche, E. Vargas, B. Valverde, and C. Diaz. Apoptotic events induced by naturally occurring retinoids ATRA and 13-cis retinoic acid on human hepatoma cell lines Hep3B and HepG2. *Cancer Lett.* **229**:271–281 (2005).
4. E. Lengfelder, S. Saussele, A. Weisser, T. Buchner, and R. Hehlmann. Treatment concepts of acute promyelocytic leukemia. *Crit. Rev. Oncol. Hematol.* **56**:261–274 (2005).
5. J. Muindi, S. R. Frankel, W. H. Jr Miller, A. Jakubowski, D. A. Scheinberg, C. W. Young, E. Dmitrovsky, and R. P. Jr Warrell. Continuous treatment with all-trans retinoic acid causes a progressive reduction in plasma drug concentrations: implications for relapse and retinoid "resistance" in patients with acute promyelocytic leukemia. *Blood* **79**:299–303 (1992).
6. B. Ozpolat, G. Lopez-Berestein, P. Adamson, C. J. Fu, and A. H. Williams. Pharmacokinetics of intravenously administered liposomal all-trans-retinoic acid (ATRA) and orally administered ATRA in healthy volunteers. *J. Pharm. Pharm. Sci.* **6**:292–301 (2003).
7. E. Estey, C. Koller, A. M. Tsimberidou, S. O'Brien, M. Beran, J. Cortes, M. Tirado-Gomez, G. Lopez-Berestein, and H. Kantarjian. Potential curability of newly diagnosed acute promyelocytic leukemia without use of chemotherapy: the example of liposomal all-*trans* retinoic acid. *Blood* **105**:1366–1367 (2005).
8. S. R. Hwang, S. J. Lim, J. S. Park, and C. K. Kim. Phospholipid-based microemulsion formulation of all-*trans*-retinoic acid for parenteral administration. *Int. J. Pharm.* **276**:175–183 (2004).
9. S. J. Lim, M. K. Lee, and C. K. Kim. Altered chemical and biological activities of all-trans retinoic acid incorporated in solid lipid nanoparticle powders. *J. Control. Release* **100**:53–61 (2004).
10. S. Kawakami, S. Suzuki, F. Yamashita, and M. Hashida. Induction of apoptosis in A549 human lung cancer cells by all-trans retinoic acid incorporated in DOTAP/cholesterol liposomes. *J. Control. Release* **110**(3):514–521 (2006).
11. S. Suzuki, S. Kawakami, N. Chansri, F. Yamashita, and M. Hashida. Inhibition of pulmonary metastasis in mice by all-*trans* retinoic acid incorporated in cationic liposomes. *J. Control. Release* **116**(1):58–63 (2006).
12. N. Chansri, S. Kawakami, F. Yamashita, and M. Hashida. Inhibition of liver metastasis by all-*trans* retinoic acid incorporated into O/W emulsions in mice. *Int. J. Pharm.* **321**:42–49 (2006).
13. V. P. Torchilin. Targeted polymeric micelles for delivery of poorly soluble drugs. *Cell Mol. Life Sci.* **61**:2549–2559 (2004).

14. G. S. Kwon. Polymeric micelles for delivery of poorly water-soluble compounds. *Crit. Rev. Ther. Drug Carr. Syst.* **20**:357–403 (2003).
15. G. Gaucher, M. H. Dufresne, V. P. Sant, N. Kang, D. Maysinger, and J. C. Leroux. Block copolymer micelles: preparation, characterization and application in drug delivery. *J. Control. Release* **109**:169–188 (2005).
16. H. Maeda. The enhanced permeability and retention (EPR) effect in tumor vasculature: the key role of tumor-selective macromolecular drug targeting. *Adv. Enzyme Regul.* **41**:189–207 (2001).
17. M. Yokoyama, T. Okano, Y. Sakurai, S. Fukushima, K. Okamoto, and K. Kataoka. Selective delivery of adriamycin to a solid tumor using a polymeric micelle carrier system. *J. Drug Target.* **7**:171–186 (1999).
18. K. Greish, T. Sawa, J. Fang, T. Akaike, and H. Maeda. SMA-doxorubicin, a new polymeric micellar drug for effective targeting to solid tumours. *J. Control. Release* **97**:219–230 (2004).
19. K. Kawano, M. Watanabe, T. Yamamoto, M. Yokoyama, P. Opanasopit, T. Okano, and Y. Maitani. Enhanced antitumor effect of camptothecin loaded in long-circulating polymeric micelles. *J. Control. Release* **112**:329–332 (2006).
20. T. Hamaguchi, Y. Matsumura, M. Suzuki, K. Shimizu, R. Goda, I. Nakamura, I. Nakatomi, M. Yokoyama, K. Kataoka, and T. Kakizoe. NK105, a paclitaxel-incorporating micellar nanoparticle formulation, can extend the therapeutic window of the drug. *Br. J. Cancer* **92**:1240–1246 (2005).
21. Y. Mizumura, Y. Matsumura, T. Hamaguchi, N. Nishiyama, K. Kataoka, T. Kawaguchi, W. J. Hrushesky, F. Moriyasu, and T. Kakizoe. Cisplatin-incorporated polymeric micelles eliminate nephrotoxicity, while maintaining antitumor activity. *Jpn. J. Cancer Res.* **92**:328–336 (2001).
22. S. Kawakami, P. Opanasopit, M. Yokoyama, N. Chansri, T. Yamamoto, T. Okano, F. Yamashita, and M. Hashida. Biodistribution characteristics of all-*trans* retinoic acid incorporated in liposomes and polymeric micelles following intravenous administration. *J. Pharm. Sci.* **94**:2606–2615 (2005).
23. P. Opanasopit, M. Yokoyama, M. Watanabe, K. Kawano, Y. Maitani, and T. Okano. Block copolymer design for camptothecin incorporation into polymeric micelles for passive tumor targeting. *Pharm. Res.* **21**:2001–2008 (2004).
24. M. Yokoyama, P. Opanasopit, T. Okano, K. Kawano, and Y. Maitani. Polymer design and incorporation methods for polymeric micelle carrier system containing water-insoluble anticancer agent camptothecin. *J. Drug Target.* **12**:373–384 (2003).
25. C. Managit, S. Kawakami, F. Yamashita, and M. Hashida. Effect of galactose density on asialoglycoprotein receptor-mediated uptake of galactosylated liposomes. *J. Pharm. Sci.* **94**:2266–2275 (2005).
26. K. Shimizu, K. Tamagawa, N. Takahashi, K Takayama, and Y Maitani. Stability and antitumor effects of all-*trans* retinoic acid-loaded liposomes contained sterylglucoside mixture. *Int. J. Pharm.* **258**:45–53 (2003).
27. G. Zuccari, R. Carosio, A. Fini, P. G. Montaldo, and I. Orienti. Modified polyvinylalcohol for encapsulation of all-*trans*-retinoic acid in polymeric micelles. *J. Control. Release* **103**:369–380 (2005).
28. Y. I. Jeong, M. K. Kang, H. S. Sun, S. S. Kang, H. W. Kim, K. S. Moon, K. L. Lee, S. H. Kim, and S. Jung. All-*trans*-retinoic acid release from core-shell type nanoparticles of poly(epsilon-caprolactone)/poly(ethylene glycol) diblock copolymer. *Int. J. Pharm.* **273**:95–107 (2004).
29. T. Takino, C. Nakajima, Y. Takakura, H. Sezaki, and M. Hashida. Controlled biodistribution of highly lipophilic drugs with various parenteral formulations. *J. Drug Target.* **1**:117–124 (1993).
30. Y. Hattori, S. Kawakami, F. Yamashita, and M. Hashida. Controlled biodistribution of galactosylated liposomes and incorporated probucol in hepatocyte-selective drug targeting. *J. Control. Release* **69**:369–377 (2000).
31. E. Ishida, C. Managit, S. Kawakami, M. Nishikawa, F. Yamashita, and M. Hashida. Biodistribution characteristics of galactosylated emulsions and incorporated probucol for hepatocyte-selective targeting of lipophilic drugs in mice. *Pharm. Res.* **21**:932–939 (2004).
32. K. Greish, J. Fang, T. Inutsuka, A. Nagamitsu, and H. Maeda. Macromolecular therapeutics: advantages and prospects with special emphasis on solid tumour targeting. *Clin. Pharmacokinet.* **42**:1089–1105 (2003).
33. N. Takahashi, K. Tamagawa, K. Shimizu, T. Fukui, and Y. Maitani. Effects on M5076-hepatic metastasis of retinoic acid and *N*-(4-hydroxyphenyl) retinamide, fenretinide entrapped in SG-liposomes. *Biol. Pharm. Bull.* **26**:1060–1063 (2003).
34. Y. Choi, S. Y. Kim, S. H. Kim, J. Yang, K. Park, and Y. Byun. Inhibition of tumor growth by biodegradable microspheres containing all-*trans*-retinoic acid in a human head-and-neck cancer xenograft. *Int. J. Cancer.* **107**:145–148 (2003).

Journal of
Nanoscience and Nanotechnology
Vol. 8, 3085–3090, 2008

Polymeric Micelles Modified by Folate-PEG-Lipid for Targeted Drug Delivery to Cancer Cells *In Vitro*

Akihiro Hayama[1], Tatsuhiro Yamamoto[2], Masayuki Yokoyama[2], Kumi Kawano[1], Yoshiyuki Hattori[1], and Yoshie Maitani[1,*]

[1]*Institute of Medicinal Chemistry, Hoshi University, 2-4-41 Ebara, Shinagawa-ku, Tokyo 142-8501, Japan*
[2]*Kanagawa Academy of Science and Technology, KSP East 404, Sakado 3-2-1, Takatsu-ku, Kawasaki-shi, Kanagawa 213-0012, Japan*

A novel technique was developed for the formation of ligand-targeted polymeric micelles that can be applicable to various ligands. For tumor-specific drug delivery, camptothecin (CPT)-loaded polymeric micelles were modified by folate to produce a folate-receptor-targeted drug carrier. Folate-linked PEG_{5000}-distearoylphosphatidylethanolamine (folate-PEG_{5000}-DSPE) was added when preparations of drug-loaded polymeric micelles, resulting in folate ligands exposed to the surface. Folate-modified CPT-loaded polymeric micelles (F-micelle) were evaluated by measuring cellular uptake using a flow cytometer, fluorescence microscopy, and confocal laser scanning microscopy, and by cytotoxicity measurement. The results revealed that F-micelle showed higher cellular uptake in KB cells over-expressing folate receptor (FR) and higher cytotoxicity compared with non-folate modified CPT-loaded polymeric micelles (plain micelles) in KB cells, but not in FR-negative HepG2 cells. This result indicated that polymeric micelles were successfully modified by the folate-linked lipid.

Keywords: Polymeric Micelles, Camptothecin, Targeting, Folate-PEG-Lipid, Folate.

RESEARCH ARTICLE

1. INTRODUCTION

Camptothecin (CPT) has shown a broad spectrum of antitumor activity;[1,2] however, its clinical use of CPT has some drawbacks, mainly due to water insolubility and aqueous instability of the lactone ring moiety. The lactone ring opens rapidly at physiological pH or above, resulting in a complete loss of biological activity.[3,4]

Nanoparticles including polymeric micelles have attracted much attention in drug delivery research. Polymeric micelles are prepared from block copolymers possessing both hydrophilic and hydrophobic chains.[5,6] Their advantageous characteristics for drug targeting include solubilization of hydrophobic molecules and high structural stability. CPT-loaded polymeric micelles enhanced the anticancer activity of CPT against solid tumors because of their prolonged blood circulation and higher accumulation in tumors.[7,8]

As with other carriers, ligand-mediated targeting of polymeric micelles to target receptors expressed selectively or over-expressed on tumor cells is increasingly recognized as an effective strategy for improving the therapeutic effect of anticancer drugs. If CPT can facilitate tumor targeting, a great contribution to the cancer chemotherapy is feasible. A variety of targeting ligands has been examined as tumor-targeted drug carriers. Folate receptor (FR) is abundantly expressed in a large percentage of human tumors, but it is only minimally distributed in normal tissue;[9] therefore, FR can serve as a functional tumor-specific receptor. Folate modification of polymeric micelles has been reported to covalently conjugate block copolymer with folate.[10,11] In these methods, the type of ligand must be decided in the preparation of polymeric micelles. In other words, the ligand-polymer conjugate must be synthesized with conformity to the drug. It is already known that a proper amount of folate-PEG-lipids could be inserted in liposomes and emulsions without change of their stability, and folate lipid-modified liposomes and emulsions with longer polyethylene glycol (PEG) linker were taken effectively by the FR-mediated cellular uptake.[12,13] However, it has been no reports about surface-modified polymeric micelles by lipid. In polymer micelles, folate might not be able to be exposed outside by steric configuration of the hydrophilic block chain. Properties of the inner core such as hydrophobicity and rigidity, were very important to achieve micelles with stable drug incorporation.[7,8,14] Folate lipid modification, therefore might affect the properties of the inner cores.

*Author to whom correspondence should be addressed.

1533-4880/2008/8/3085/006 doi:10.1166/jnn.2008.093

For targeted drug delivery to cancer cells, we prepared folate-modified CPT-loaded polymeric micelles (F-micelle), and evaluated by measuring cellular uptake using a flow cytometer, fluorescence microscopy, and confocal laser scanning microscopy, and by cytotoxicity measurement. In this paper, we describe a novel method of folate modification to CPT-loaded polymeric micelles by folate-linked PEG_{5000}-distearoylphosphatidylethanolamine (folate-PEG_{5000}-DSPE).

2. MATERIALS AND METHODS

2.1. Materials

Poly(ethylene glycol)-poly(benzyl aspartate-53) block copolymer (PEG-P(Asp(Bz53))) was synthesized as described previously.[14, 15] The molecular weight of the PEG block was 2000 and the average number of aspartate units was 17. Fifty-three percentage of the aspartic acid residue was esterified with the benzyl group. CPT and folic acid were purchased from Wako Pure Chemicals (Tokyo, Japan). Folate-PEG_{5000}-DSPE was synthesized as described previously.[12, 13] 1,1′-Dioctadecyl-3,3,3′,3′-tetramethylindocarbocyanine perchlorate (DiI) was purchased from Lambda Probes and Diagnostics (Graz, Austria).

2.2. Preparation of Folate-Modified CPT-Loaded Polymeric Micelles (F-Micelles)

CPT was incorporated into polymeric micelles by an evaporation method as described previously,[15] using 0.5 mg of CPT, 5 mg of block copolymer, and 0 mol%, 0.03 mol% (0.027 mg), 0.1 mol% (0.092 mg) and 0.2 mol% (0.18 mg) of folate-PEG_{5000}-DSPE to CPT loaded in micelles for plain micelles, 0.03F-micelle, 0.1F-micelle and 0.2F-micelle, respectively. DiI-labeled F-micelles were prepared by the same protocol, but with the post-addition of DiI at 0.4 mol% of incorporated CPT. The incorporation efficiency was calculated as described previously.[15] The mean particle diameters and ζ-potentials were determined using a particle size analyzer (ELS-Z, Otsuka Electronics, Osaka, Japan) at 25 °C by diluting the dispersion to an appropriate volume with water.

2.3. *In Vitro* Drug Release

Release of CPT in F-micelles from a dialysis tube was measured using seamless cellulose tube membranes (Viskase Sales Corp., IL, USA) with a molecular cut-off of 12,000–14,000. The initial concentration of CPT was 10 μg/ml. The sample volume in the dialysis bag was 1 ml and the sink volume was 200 ml PBS at pH 7.4 with the medium at 37 ± 0.1 °C. The drug concentration was analyzed using fluorescence spectrophotometer F-4010 (Hitachi, Tokyo, Japan) (excitation 369 nm, emission 426 nm).

2.4. Cell Culture

KB cells (FR (+)) and HepG2 cells (FR (−)) were obtained from the Cell Resource Center for Biomedical Research, Tohoku University (Miyagi, Japan). Both cells were cultured in folate-deficient RPMI 1640 medium (Invitrogen Corp., Carlsbad, CA, USA) with 10% heat-inactivated fetal bovine serum (Invitrogen Corp.) and 100 μg/ml kanamycin with 5% CO_2 at 37 ° C.

2.5. Flow Cytometry Analysis

KB cells were prepared by plating 5×10^5 cells in a 6-well culture plate 1 day before the assay. Cells were incubated with DiI-labeled F-micelles containing 10 μg CPT/ml diluted in 2 ml folate-deficient RPMI 1640 medium for 2 hours at 37 °C. In free-folic acid competition studies, 2 mM folic acid was added to the medium. After incubation, cells were washed two times with acidic saline (pH 3) followed by one wash with cold phosphate-buffered saline (PBS, pH 7.4) to remove unbound polymeric micelles, detached with 0.02% EDTA-PBS, and then suspended in PBS containing 0.1% bovine serum albumin and 1 mM EDTA. The suspended cells were directly introduced to a FACSCalibur flow cytometer (Becton Dickinson, San Jose, CA, USA) equipped with a 488 nm argon ion laser. Data for 10,000 fluorescent events were obtained by recording forward scatter, side scatter, and 585/42 nm fluorescence. The autofluorescence of cells was taken as a control.

2.6. Fluorescence and Confocal Laser Scanning Microscopy

After incubation, cells were washed as described above; 2 ml fresh medium was added. The cells were observed with fluorescence microscopy (ECLIPSE TS100, Nikon, Tokyo, Japan) at just. For confocal laser scanning microscopy, cells were fixed with Mildform 20 N for 30 min at room temperature. Subsequently, the cells were washed three times with PBS. Examinations were performed with a Radiance 2100 confocal laser-scanning microscope (BioRad, CA, USA).

2.7. Cytotoxicity Study

Cells were prepared by plating 1×10^4 cells in a 96-well culture plate 1 day before the experiment. KB and HepG2 cells were then incubated for 2 hours at 37 °C with 100 μl CPT solution, plain micelle, and F-micelles (containing 0.01, 0.1, 0.5, 1, 2.5 and 5 μg CPT) diluted in folate-deficient RPMI 1640 medium. The medium was replaced with fresh medium and incubated for a further 48 hours. Cytotoxicity was determined with the WST-8 assay (Dojindo Laboratories, Kumamoto, Japan). The number of viable cells was then determined by absorbance measured at 450 nm on an automated plate reader (BioRad, CA, USA).

RESEARCH ARTICLE

2.8. Statistical Analysis

Statistical comparisons were performed by Student's t-test. P values less than 0.05 were considered significant.

3. RESULTS AND DISCUSSION

3.1. Determination of CPT Content and Particle Size of F-Micelles

In our previous study, folate modification with a sufficiently long PEG chain on emulsion is an effective way of targeting drug carriers to tumor cells.[13] Therefore, folate-lipid conjugate with PEG_{5000} linker was used for the modification of polymeric micelles with PEG_{2000}. Four kinds of CPT-loaded polymeric micelles were formulated as plain micelles, 0.03F-micelle, 0.1F-micelle and 0.2F-micelle. Folate-PEG-DSPE may be incorporated to polymeric micelles since 0.2 mol% folate-PEG_{5000}-DSPE was 9.6 μM, and the critical micelle concentration (CMC) value of folate-PEG_{5000}-DSPE was 12.1 μM determined by the fluorescence probe technique using DiI.

The average particle size of each F-micelle in water was about 230 nm with 0.5–1.1 mV in ζ-potential and the CPT-loading efficiency was about 50%. These values of F-micelles did not change significantly compared with plain micelles.

3.2. *In Vitro* Drug Release

The *in vitro* release of CPT from 0.03F-micelle exhibited rapid release behavior in an early stage (about 40% in 2 hours, Fig. 1). In contrast, the release of CPT from 0.2F-micelle and plain micelles reached only about 20% after the same period of incubation. This result indicates that the quantity of folate modification affected the stability of polymeric micelles, indicating that the higher the folate surface density, the lower the drug release. Similar results were reported that folate modification of liposomes influenced the release pattern.[16] The decreased drug release from highly folate-modified polymer micelles might be due to the structural integrity of folate coupling, that may lead to barrier effect for CPT diffusion.

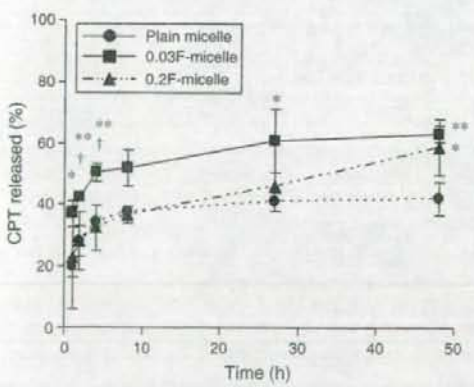

Fig. 1. Release profiles from plain and folate-modified CPT-loaded polymeric micelles at 37 °C in PBS as a sink solution at pH = 7.4. Each value represents the mean ± S.D. ($n = 3$). $^{*}P < 0.05$, $P < 0.01$ compared with plain micelle. $^{\dagger}P < 0.05$ compared with 0.2F-micelle.

3.3. Uptake of F-Micelles to KB Cells

Cellular uptake of F-micelle was evaluated using polymeric micelles labeled with DiI by flow cytometry. The fluorescence of 10 μg CPT/ml of DiI-labeled plain

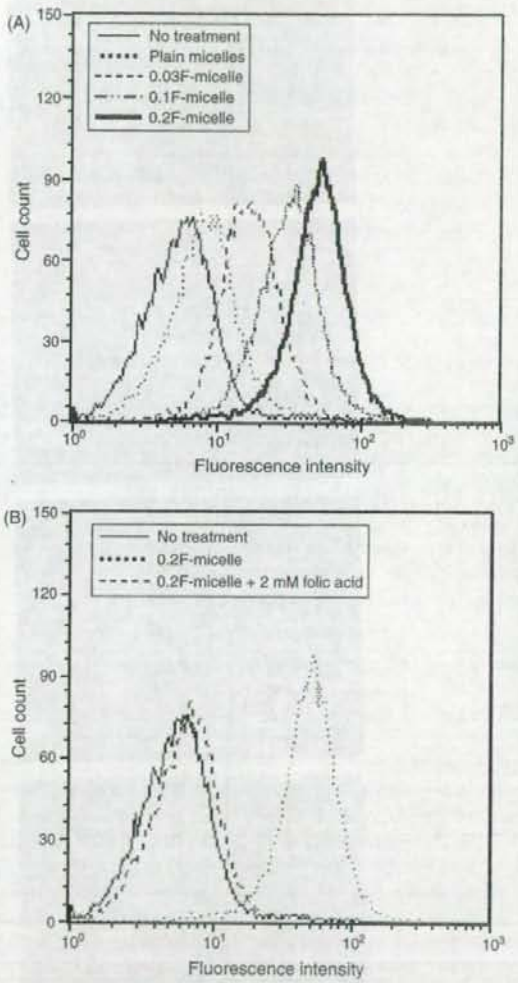

Fig. 2. Uptake of DiI-labeled plain and folate-modified CPT-loaded polymeric micelles with KB cells in the absence (A), or presence of 2 mM folic acid (B). Cells were incubated with polymeric micelles in folate-free RPMI 1640 medium for 2 hours at 37 °C and analyzed by flow cytometry. No treatment indicates autofluorescence of untreated cells. Each analysis was generated by counting 10^4 cells.

RESEARCH ARTICLE

micelles and F-micelles showed almost identical spectrofluorimetric units (data not shown). As shown in Figure 2(A), flow cytometry analysis represented a shift in the curve. 0.2F-micelle indicated higher mean intensity of about 13.8-fold, 7.9-fold and 3.3-fold in cellular association of plain micelles, 0.03F-micelle and 0.1F-micelle after 2 hours exposure, respectively. In contrast, micelles modified with methoxy-PEG_{5000}-DSPE showed a similar curve to plain micelles (data not shown). Additionally, these increased associations of 0.03F-micelle, 0.1F-micelle (data not shown) and 0.2F-micelle could be completely blocked by adding 2 mM folic acid to the medium (Fig. 2(B)). This is the first report showing that folate-lipid was incorporated and its folate group was exposed on the surface of polymeric micelles to interact with FR. The results also indicate that F-micelle was transported within cells by an FR-mediated endocytosis process. These findings are consistent with those reported previously on the FR-mediated cellular uptake of folate-modified liposomes and emulsions for anti-cancer therapy.[12, 13]

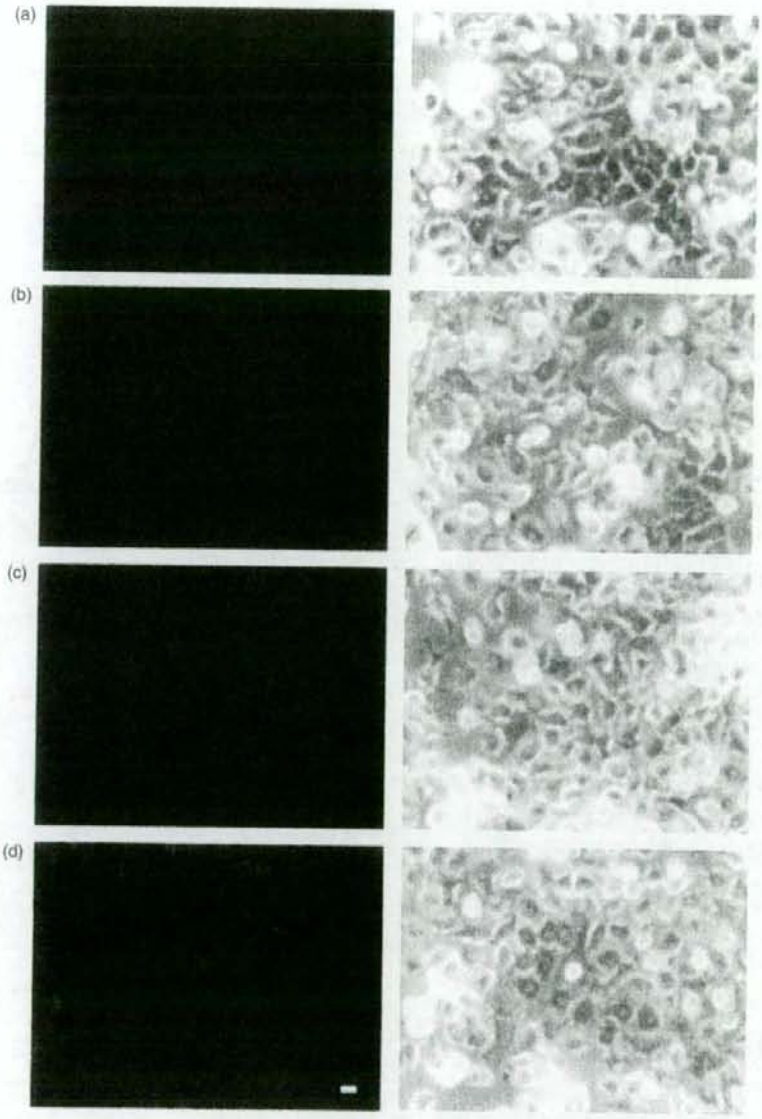

Fig. 3. Fluorescence microscopic images of KB cells treated with (a) plain micelles, (b) 0.03F-micelle, (c) 0.1F-micelle and (d) 0.2F-micelle. Cells were incubated with polymeric micelles in folate-free RPMI 1640 medium for 2 hours at 37 °C, then observed just after. (×200) Scale bar denotes 10 μm.

RESEARCH ARTICLE

Cellular uptake of F-micelles was also evaluated using fluorescence microscopy. Fluorescence images of KB cells after incubation with F-micelles for 2 hours are shown in Figure 3. For plain micelles, there was no remarkable uptake in fluorescent intensity of KB cells. In contrast, in F-micelles, more fluorescently labeled cells could be clearly visualized, and 0.2F-micelle was especially taken up in to the cells. This result is similar to that of flow cytometry. In accordance with the results from flow cytometry analysis, fluorescence microscopy confirmed that F-micelles could be targeted to cancer cells over-expressing FR on their surface.

3.4. Localization of F-Micelles to KB Cells

To investigate whether F-micelles existed on cell surface or within cells, localization of F-micelles was evaluated using confocal laser scanning microscopy. Fluorescence images of KB cells after incubation with 0.03F-micelle for 2 hours are shown in Figure 4. 0.2F-micelle showed similar image (data not shown). The localization of DiI-labeled F-micelles was confirmed by changing the Z-axis of observed area with 1 μm. DiI-fluorescence was detected as punctuate dots within cells. This indicated that F-micelles were internalized into the cells and located within endosome compartments.

3.5. Cytotoxicity Study

FR-targeted polymeric micelles were evaluated for *in vitro* cytotoxicity in FR (+) KB and FR (−) HepG2 cells by WST-8 assay. Superior cytotoxicity of F-micelles over plain micelles was observed in KB cells, but not in HepG2 cells. IC_{50} values for KB cells of F-micelles were about 2–3 times lower than the plain micelles (Table I). The difference of IC_{50} values between 0.03F-micelle and 0.2F-micelle was not large. It might be due to the release of CPT from 0.03F-micelle was faster than that from 0.2F-micelle, and free CPT was taken up to the cells as well as micelles. In contrast, IC_{50} values for HepG2 cells show hardly any difference between F-micelles and plain micelles.

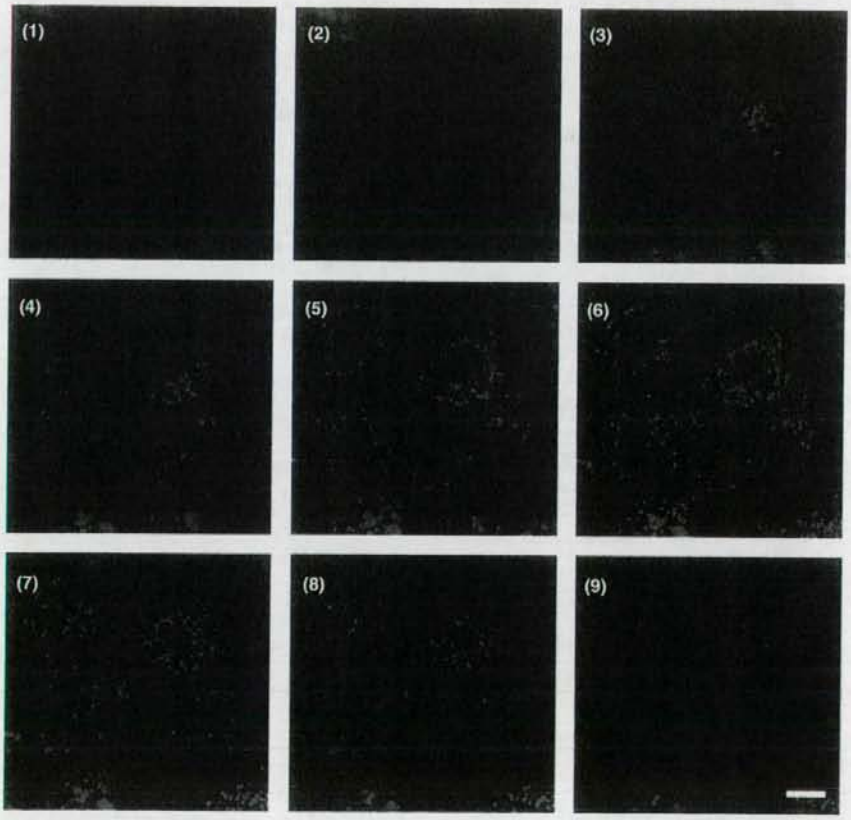

Fig. 4. Localization of DiI-labeled folate-modified CPT-loaded polymeric micelles (0.03F-micelle) with KB cells. Cells were incubated with polymeric micelles in folate-free RPMI 1640 medium for 2 hours at 37 °C, then observed just after under confocal laser scanning microscopy by changing the Z-axis. Images (1–9) represent regular intervals of 1 μm on the Z-axis from bottom to top cells, respectively. (×1200) Scale bars denote 10 μm.

RESEARCH ARTICLE

Table I. IC_{50} value (μg/ml) of CPT solution, plain micelles, folate-modified CPT-loaded polymeric micelles for KB cells and HepG2 cells.

		Polymeric micelles			
Cells	CPT-solution	Plain	0.03F	0.1F	0.2F
KB	3.0±0.4	6.7±1.1	2.2±0.5	3.6±0.8	2.1±0.9
HepG2	2.2±0.2	8.7±0.9	8.4±0.4	7.4±1.0	6.5±1.6

Data are shown as the mean ± S.D. ($n = 3$).

The CPT lactone ring opened at about 20 minutes in medium.[3] The lactone E-ring in CPT plays an important role in a drug's biological activity but it exists in a pH-dependent equilibrium in an open ring carboxylate form. Incorporation of CPT in micelles could maintain active lactone form even in the presence of serum,[14] indicating that micelle formulations could keep the antitumor effect of CPT. Plain micelles showed lower cytotoxicity than CPT solution, because the PEG shells of polymeric micelles inhibited interaction with cells. However, folate modification of polymeric micelles increased the association with cells via FR, resulting in increase of the cytotoxicity similar to CPT solution. It is one of the reasons that IC_{50} values of F-micelles were much higher or similar to those for CPT solution. Preferential partitioning of the lactone form into lipid layers has been previously reported to stabilize CPT.[3,17] *In vivo* situation, micelle formulation enhanced the accumulation in tumor tissue than CPT solution.[8] Further interaction of folate may increase the antitumor effect of CPT micelles. These results indicate that 0.2F-micelle is suitable drug carrier for selective drug delivery and is more adapted than 0.03F-micelle.

4. CONCLUSION

Uptake and cytotoxicity study showed that F-micelles could be selectively taken into cancer cells by folate-receptor mediated endocytosis. The novel lipid-based modification method to polymeric micelles is applicable to antibody, peptides, or other ligands. Furthermore, this allows double targeting using folate-lipid and another ligand-conjugated polymeric micelles or folate-targeted therapeutics to be tailored to the needs of individual patients.

Acknowledgments: This work was supported by Grants-in-Aids from the Ministry of Health, Labour and Welfare of Japan, and by Open Research Center Project. We are grateful to Mr. Atsushi Yamada and Mr. Takashi Yoshizawa for providing folate-PEG_{5000}-DSPE.

References and Notes

1. B. C. Giovanella, H. R. Hinz, A. J. Kozielski, J. S. Stehlin, Jr., R. Silber, and M. Potmesil, *Cancer Res.* 51, 3052 (**1991**).
2. B. C. Giovanella, J. S. Stehlin, M. E. Wall, M. C. Wani, A. W. Nicholas, L. F. Liu, R. Silber, and M. Potmesil, *Science* 246, 1046 (**1989**).
3. T. G. Burke, A. E. Staubus, and A. K. Mishra, *J. Am. Chem. Soc.* 114, 8318 (**1992**).
4. J. Fassberg and V. J. Stella, *J. Pharm. Sci.* 81, 676 (**1992**).
5. K. Kataoka, A. Harada, and Y. Nagasaki, *Adv. Drug Deliv. Rev.* 47, 113 (**2001**).
6. V. P. Torchilin, *Mol. Life Sci.* 61, 2549 (**2004**).
7. M. Watanabe, K. Kawanos, M. Yokoyama, P. Opanasopit, T. Okano, and Y. Maitani, *Int. J. Pharm.* 308, 183 (**2006**).
8. K. Kawano, M. Watanabe, T. Yamamoto, M. Yokoyama, P. Opanasopit, T. Okano, and Y. Maitani, *J. Control. Release* 112, 329 (**2006**).
9. M. Wu, M. Gunning, and M. Ratnam, *Biomarkers Prev.* 8, 775 (**1999**).
10. P. V. Paranjpe, Y. Chen, V. Kholodovych, W. Welsh, S. Stein, and P. J. Sinko, *J. Control. Release* 100, 275 (**2004**).
11. H. S. Yoo and T. G. Park, *J. Control. Release* 96, 273 (**2004**).
12. A. Gabizon, A. T. Horowitz, D. Goren, D. Tzemach, F. Mandelbaum-Shavit, M. M. Qazen, and S. Zalipsky, *Bioconjug. Chem.* 10, 289 (**1999**).
13. T. Shiokawa, Y. Hattori, K. Kawano, Y. Ohguchi, H. Kawakami, K. Toma, and Y. Maitani, *Clin. Cancer Res.* 11, 2018 (**2005**).
14. P. Opanasopit, M. Yokoyama, M. Watanabe, K. Kawano, Y. Maitani, and T. Okano, *Pharm. Res.* 21, 2001 (**2004**).
15. M. Yokoyama, P. Opanasopit, T. Okano, K. Kawano, and Y. Maitani, *J. Drug Target.* 12, 373 (**2004**).
16. Y. Gupta, A. Jain, P. Jain, and S. Jain, *J. Drug Target.* 15, 231 (**2007**).
17. Y. Sadzuka, S. Hirotsu, and S. Hirota, *Jpn. J. Cancer Res.* 90, 226 (**1999**).

Received: 20 June 2007. Accepted: 8 August 2007.

RESEARCH ARTICLE

+Model
IJP-10028; No. of Pages 5

Available online at www.sciencedirect.com
ScienceDirect
International Journal of Pharmaceutics xxx (2008) xxx–xxx
INTERNATIONAL JOURNAL OF PHARMACEUTICS
www.elsevier.com/locate/ijpharm

Note

Block copolymer design for stable encapsulation of *N*-(4-hydroxyphenyl)retinamide into polymeric micelles in mice

Tomoyuki Okuda [a], Shigeru Kawakami [a], Masayuki Yokoyama [b], Tatsuhiro Yamamoto [b], Fumiyoshi Yamashita [a], Mitsuru Hashida [a,*]

[a] *Department of Drug Delivery Research, Graduate School of Pharmaceutical Sciences, Kyoto University, Sakyo-ku, Kyoto 606-8501, Japan*
[b] *Kanagawa Academy of Science and Technology, KSP East 404, Sakado 3-2-1, Takatsu-ku, Kawasaki-shi, Kanagawa 213-0012, Japan*

Received 5 October 2007; received in revised form 22 January 2008; accepted 24 January 2008

Abstract

For stable encapsulation of *N*-(4-hydroxyphenyl)retinamide (4-HPR) into polymeric micelles, four types of block copolymers were synthesized with different esterified functional groups: heptyl (C7), nonyl (C9), benzyl (Bz), and phenylpropyl (C3Ph). The stability of 4-HPR encapsulated polymeric micelles was evaluated by measuring the blood concentration of 4-HPR in mice. After intravenous administration of 4-HPR and 4-HPR encapsulated PEG liposomes, the blood concentration of 4-HPR was about 2.8% and 2.2% of the dose/mL, suggesting the rapid release of 4-HPR from PEG liposomes. In contrast, the blood concentration of 4-HPR after intravenous administration of all 4-HPR encapsulated polymeric micelles studied was much higher (about 22–34% of the dose/mL). Among them, the polymeric micelles prepared by block copolymers (Bz) showed the highest blood concentration of 4-HPR. As far as the effects of the level of Bz groups in the block copolymers are concerned, the blood concentration of 4-HPR was enhanced by Bz groups at a level of 72% and 77%, but not by Bz groups at a level of 43% and 51%. These results suggest that 4-HPR is stably encapsulated in polymeric micelles prepared by block copolymers (Bz) but a level of over 72% of Bz groups is needed. These findings will be of value in the future use, design, and development of polymeric micelles for *in vivo* application of 4-HPR.

Keywords: 4-HPR; Fenretinide; Polymeric micelle; Controlled release; Drug delivery systems

N-(4-Hydroxyphenyl)retinamide (4-HPR, fenretinide) is a synthetic retinoid which shows high anti-tumor activity against a variety of malignant cells (Formelli et al., 1996). Although oral administration of 4-HPR has been used in clinical trials so far, its bioavailability is very limited because of its low membrane permeability (Kokate et al., 2006). In addition, intravenous 4-HPR is rapidly eliminated from body (Swanson et al., 1980; Hultin et al., 1986). Therefore, 4-HPR cannot exert a high enough anti-tumor activity because its low blood concentration (Formelli et al., 1993). Raffaghello et al. and Takahashi et al. have reported that 4-HPR encapsulated liposomes containing monoclonal antibody or sterylglucoside mixture exert anti-tumor activities when given intravenously. Therefore, the development of a targeting carrier for 4-HPR is needed in order to obtain potent *in vivo* anti-tumor activity (Raffaghello et al., 2003; Takahashi et al., 2003).

Polymeric micelles prepared by block copolymers, which are composed of both hydrophilic and hydrophobic segments, have been reported to be suitable drug carriers for lipophilic drugs (Kataoka et al., 2001; Gaucher et al., 2005). Recently, we have reported the efficient encapsulation of hydrophobic drugs in polymeric micelles by optimizing the hydrophobic segments with esterified functional groups of poly(ethylene glycol)–poly(aspartate ester) block copolymers (Yokoyama et al., 2004; Kawakami et al., 2005; Watanabe et al., 2006; Chansri et al., 2008). These observations prompted us to investigate the potential use of polymeric micelle formulations by optimizing the hydrophobic segments with esterified functional groups to enhance the blood retention of 4-HPR following intravenous administration. Here, four types of poly(ethylene glycol)–poly(aspartate ester) block copolymers with different esterified functional groups were synthesized to optimize the

* Corresponding author. Tel.: +81 75 753 4545; fax: +81 75 753 4575.
E-mail address: hashidam@pharm.kyoto-u.ac.jp (M. Hashida).

0378-5173/$ – see front matter © 2008 Elsevier B.V. All rights reserved.
doi:10.1016/j.ijpharm.2008.01.044

Please cite this article in press as: Okuda, T., et al., Block copolymer design for stable encapsulation of *N*-(4-hydroxyphenyl)retinamide into polymeric micelles in mice, Int J Pharm (2008), doi:10.1016/j.ijpharm.2008.01.044

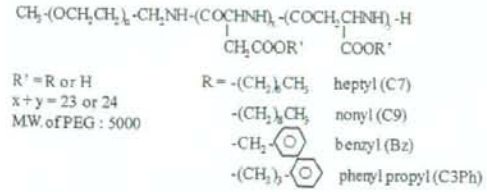

Fig. 1. Schematic illustration of synthesized block copolymers.

stable encapsulation of 4-HPR in the inner core of polymeric micelles (Fig. 1).

Since the *in vivo* drug release from particulate carriers is much higher than that from *in vitro* drug release (Takino et al., 1993; Shabbits et al., 2002), *in vivo* evaluation is important for the development of polymeric micelles for 4-HPR encapsulation. Therefore, the blood concentration of 4-HPR following intravenous administration of 4-HPR encapsulated polymeric micelles into the tail vein of mice was measured using HPLC.

Poly(ethylene glycol)–poly(aspartate ester) block copolymers were obtained by an esterification reaction between a bromide compound and the aspartic acid residue of poly(ethylene glycol)–poly(aspartic acid) block copolymers (Yokoyama et al., 2004). Block copolymers with heptyl, nonyl, benzyl and phenyl propyl groups are abbreviated as C7, C9, Bz and C3Ph, respectively. The esterification level determined by ^{1}H NMR is expressed as a % value following the block copolymer abbreviation. 4-HPR encapsulated polymeric micelles were prepared by a conventional evaporation method modified as described in our previous report (Kawakami et al., 2005). The ratio of block copolymers/4-HPR for their preparation was fixed as 2.5 (weight ratio). As a control, poly(ethylene glycol) modified liposomes (PEG liposomes) were selected to evaluate the potentials of novel polymeric micelle formulations because of their wide use in cancer chemotherapy (Torchilin, 2005).

The physicochemical properties, such as the particle size and zeta potential of the macromolecules, are determining factors for their biodistribution (Takakura and Hashida, 1996). For escape

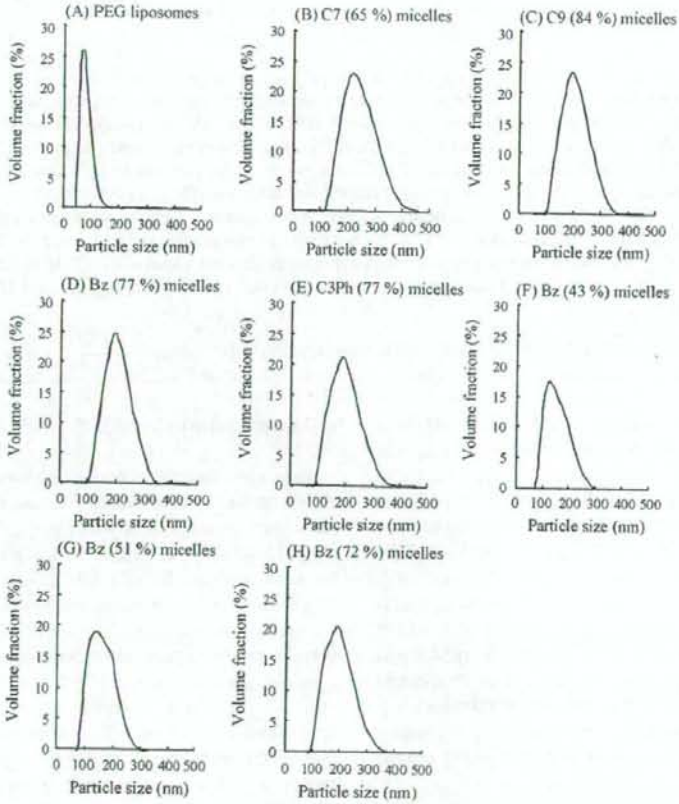

Fig. 2. Size distribution of 4-HPR encapsulated PEG liposomes (A) and polymeric micelles with several types and levels of esterified functional groups (B–H). 4-HPR encapsulated PEG liposomes were composed of hydrogenated soybean phosphatidyl choline (HSPC), cholesterol, distearoylphosphatidylethanolamine-*N*-[methoxy(polyethylene glycol)-2000] (PEG-DSPE), and 4-HPR (33.3:16.7:1.67:1, molar ratio). The ratio of block copolymers/4-HPR for 4-HPR encapsulated polymeric micelles was fixed as 2.5 (weight ratio). They were prepared by a conventional evaporation method modified as described in our previous report (Kawakami et al., 2005).

Please cite this article in press as: Okuda, T., et al., Block copolymer design for stable encapsulation of *N*-(4-hydroxyphenyl)retinamide into polymeric micelles in mice, Int J Pharm (2008), doi:10.1016/j.ijpharm.2008.01.044

Table 1
Zeta potential of 4-HPR encapsulated PEG liposomes (A) and polymeric micelles with several types and levels of esterified functional groups (B–H)

Carrier	Zeta potential (mV)
(A) PEG liposomes	−2.7 ± 1.4
(B) C7 (65%) micelles	−1.7 ± 0.7
(C) C9 (84%) micelles	−2.6 ± 1.0
(D) Bz (77%) micelles	−1.4 ± 1.2
(E) C3Ph (77%) micelles	−0.8 ± 0.8
(F) Bz (43%) micelles	−10.7 ± 1.8
(G)Bz (51%) micelles	−3.1 ± 0.9
(H) Bz (72%) micelles	−2.3 ± 3.2

Each value represents the means ± S.D. (n = 3–4).

of uptake by the reticuloendothelial system and long-term blood retention in the systemic circulation, it is needed that the particle size and zeta potential of PEG modified particulates (liposomes and polymeric micelles) are about <200 nm and weak anion (Oku and Namba, 1994; Nishiyama et al., 2003). Therefore, the mean particle size and zeta potential of 4-HPR encapsulated polymeric micelles were measured using Zetasizer Nano Series (Malven Instruments Ltd., Worcestershire, UK). As shown in Fig. 2 and Table 1, the mean particle size and zeta potential of all 4-HPR encapsulated polymeric micelles ranged from 142 to 225 nm and from −10.7 to −0.8 mV respectively, not dramatically changed irrespective of types and levels of esterified functional groups. The mean particle size and zeta potential of 4-HPR encapsulated PEG liposomes were about 76 nm and −2.7 mV. Thus, 4-HPR encapsulated polymeric micelles and PEG liposomes can avoid uptake by the reticuloendothelial system and enhance the blood retention of 4-HPR after intravenous administration.

After intravenous administration of 4-HPR itself (dissolved in polyoxyethylene hydrogenated castor oil (HCO-60), which was a solubilizing agent) and 4-HPR encapsulated PEG liposomes at 1 h, the blood concentration of 4-HPR was about 2.8% and 2.2% of the dose/mL (Fig. 3), suggesting the rapid release of 4-HPR from PEG liposomes. From the reports of Swanson et al. (1980) and Hultin et al. (1986), the blood concentration of 4-HPR at 1 h after intravenous injection was calculated to be about 3% of the dose/mL, supporting our result. In contrast, the blood concentration of 4-HPR was about 22–34% of the dose/mL after intravenous administration of 4-HPR encapsulated polymeric micelles, suggesting the stable encapsulation of 4-HPR by these types of polymeric micelles. Among them, the polymeric micelles prepared by block copolymers (Bz (77%)) exhibited the highest blood concentration of 4-HPR. Recently, Kataoka et al. reported that doxorubicin can be stably encapsulated in polymeric micelles prepared by poly(ethylene glycol)–poly(β-benzyl-L-aspartate) block copolymers through π–π stacking (Kataoka et al., 2000). Therefore, 4-HPR, which possesses a benzene ring, might be also stably encapsulated in polymeric micelles prepared by block copolymers (Bz (77%)) through this π–π stacking. As far as the effects of the level of Bz groups in the block copolymers are concerned, the blood concentration of 4-HPR was enhanced by Bz groups at a level of 72% and 77%, but not by Bz groups at a level of 43% and 51% (Fig. 4). These results suggest that 4-HPR is stably encapsulated in polymeric micelles prepared by block copolymers (Bz) although a level of over 72% of Bz groups in block copolymers is needed.

Furthermore, long-term biodistribution of 4-HPR after intravenous injection of 4-HPR encapsulated polymeric micelles prepared by block copolymers (Bz (77%)) was evaluated. After intravenous injection of 4-HPR itself (dissolved in HCO-60), 4-HPR was rapidly eliminated from blood circulation and highly distributed in liver (Fig. 5). In addition, all of tissue to blood concentration ratio (K_p) of 4-HPR were increased as time passed, especially K_p value on kidney at 8 h was most high compared with other tissues (Fig. 6). These trends were supported by other report with different intravenous formulation of 4-HPR (Swanson et al., 1980). On the other hand, 4-HPR encapsulated polymeric micelles prepared by block copolymers (Bz (77%)) showed much higher blood concentration of 4-HPR for more than 8 h and lower liver distribution of 4-HPR until 1 h compared with 4-HPR itself (Fig. 5). These results indicated that, 4-HPR encapsulated polymeric micelles prepared by block copolymers (Bz (77%)) showed prolonged circulation of 4-HPR for stable encapsulation of 4-HPR and escape of initial uptake by liver. The mean area under the curve ($AUC_{0-8\,h}$) in blood of 4-HPR itself

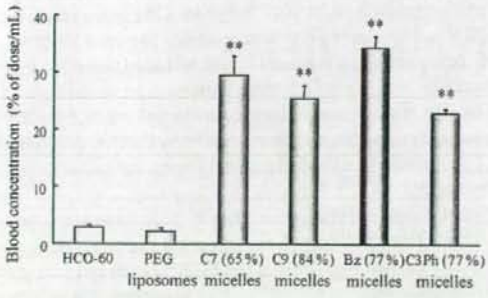

Fig. 3. Blood concentration of 4-HPR itself (dissolved in HCO-60), 4-HPR encapsulated in PEG liposomes, and in polymeric micelles with several types of esterified functional groups at 1 h after intravenous injection into mice at a dose of 5 mg/kg as 4-HPR. Each value represents the means ± S.D. (n = 3–4). **P < 0.01, compared with HCO-60 groups.

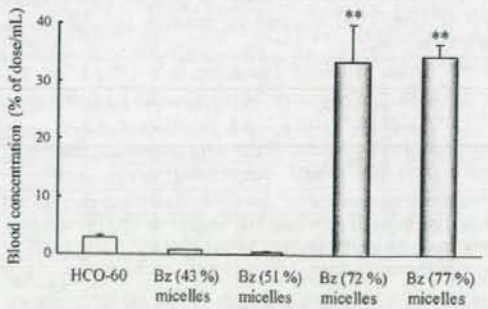

Fig. 4. Effect of level of Bz groups in block copolymers on blood concentration of 4-HPR encapsulated in Bz micelles at 1 h after intravenous injection into mice at a dose of 5 mg/kg as 4-HPR. Each value represents the means ± S.D. (n = 3–4). **P < 0.01, compared with HCO-60 groups.

Please cite this article in press as: Okuda, T., et al., Block copolymer design for stable encapsulation of *N*-(4-hydroxyphenyl)retinamide into polymeric micelles in mice, Int J Pharm (2008), doi:10.1016/j.ijpharm.2008.01.044

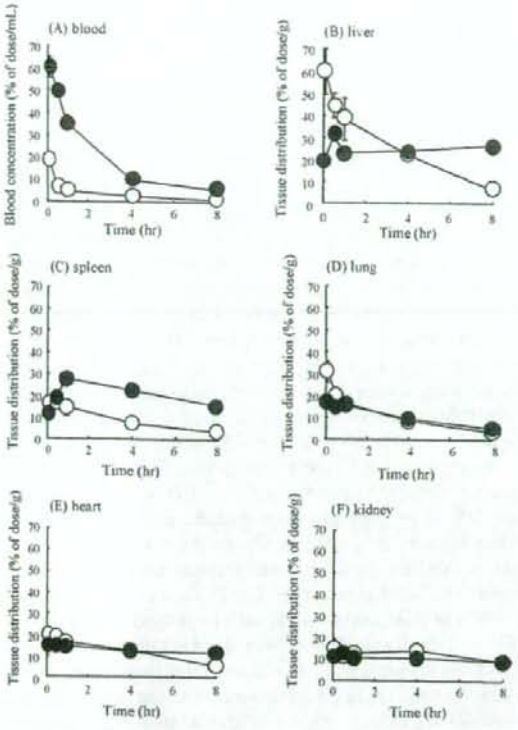

Fig. 5. Blood concentration (A) or tissue accumulation (liver (B), spleen (C), lung (D), heart (E), kidney (F)) of 4-HPR itself (dissolved in HCO-60) (○) and 4-HPR encapsulated in Bz (77%) micelles (●) after intravenous injection into mice at a dose of 5 mg/kg as 4-HPR. Each value represents the mean ± S.D. (n = 3–4).

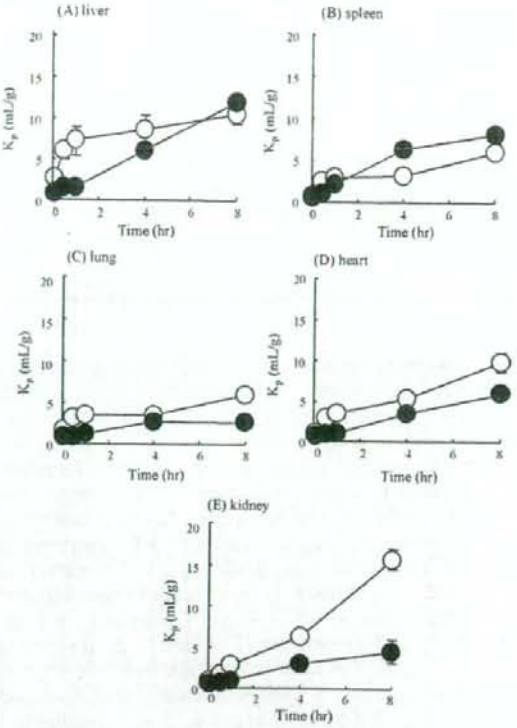

Fig. 6. Tissue to blood concentration ratio (K_p) of 4-HPR in liver (A), spleen (B), lung (C), heart (D), and kidney (E) of 4-HPR itself (dissolved in HCO-60) (○) and 4-HPR encapsulated in Bz (77%) micelles (●) after intravenous injection into mice at a dose of 5 mg/kg as 4-HPR. Each value represents the mean ± S.D. (n = 3–4).

and 4-HPR encapsulated in Bz (77%) micelles calculated by the linear trapezoidal rule was 26.4 and 148 (% of dose × h/mL) and its relative AUC ratio was 5.6. Furthermore, K_p in lung, heart, and kidney after intravenous injection of 4-HPR encapsulated polymeric micelles prepared by block copolymers (Bz (77%)) were lower than that of 4-HPR itself (Fig. 6), suggesting that, 4-HPR encapsulated polymeric micelles prepared by block copolymers (Bz (77%)) escaped the transition of 4-HPR from blood to these tissues.

In this study, enhanced blood retention of 4-HPR was achieved by using polymeric micelles prepared by poly(ethylene glycol)–poly(aspartate ester) block copolymers, which were optimized hydrophobic segments with esterified functional groups. In particular, 4-HPR encapsulated polymeric micelles prepared by block copolymers (Bz (77%)) had the highest blood concentration of 4-HPR, which was about 106 μM (34% of the dose/mL) at a dose of 5 mg/kg. As far as the pharmacological effects of 4-HPR on cancer cells are concerned, Kalemkerian et al. have reported that 4-HPR efficiently inhibited the growth of small-cell lung cancer cell line and its IC_{50} values ranged from 0.1 to 3.0 μM (Kalemkerian et al., 1995). The neovascularization formed by solid tumors exhibits some unique features, such as hypervasculature, leaky capillaries and poor lymphatic clearance. These characteristics cause the accumulation of macromolecules in tumors for a long period, known as enhanced permeability and retention (EPR) effects (Matsumura and Maeda, 1986). The spaces in the blood endothelium formed by solid tumors are reported to range from 300 to 4700 nm (Yuan et al., 1995; Hashizume et al., 2000). Since the mean diameter of 4-HPR encapsulated polymeric micelles prepared by block copolymers (Bz (77%)) is about 175 nm, and maximally 342 nm, these may be small enough to pass through the endothelium of solid tumors. These observations led us to believe that 4-HPR encapsulated polymeric micelles prepared by block copolymers (Bz (77%)) could be effective carrier systems for use in future cancer therapy.

In conclusion, poly(ethylene glycol)–poly(aspartate ester) block copolymers with heptyl, nonyl, benzyl and phenyl propyl groups (abbreviated as C7, C9, Bz and C3Ph) were synthesized for stable encapsulation of 4-HPR. It is suggested that 4-HPR is stably encapsulated in polymeric micelles prepared by block copolymers (Bz) although a level of over 72% of Bz groups in the block copolymers is needed for stable encapsulation of 4-HPR. The information we have obtained in this study will be of

Please cite this article in press as: Okuda, T., et al., Block copolymer design for stable encapsulation of *N*-(4-hydroxyphenyl)retinamide into polymeric micelles in mice, Int J Pharm (2008), doi:10.1016/j.ijpharm.2008.01.044

value for the future use, design, and development of polymeric micelles involving the *in vivo* application of 4-HPR.

Acknowledgements

This work was supported in part by Grants-in-Aid for Scientific Research and the Program for Promoting the Establishment of Strategic Research Centers, Special Coordination Funds for Promoting Science and Technology from the Ministry of Education, Culture, Sports, Science, and Technology of Japan, and by the Health and Labour Sciences Research Grants for Research on Advanced Medical Technology from the Ministry of Health, Labour and Welfare of Japan. Yokoyama M. and Yamamoto T. acknowledge support by the Program for Promoting the Establishment of Strategic Research Centers, Special Coordination Funds for Promoting Science and Technology from the Ministry of Education, Culture, Sports, Science, and Technology of Japan.

References

Chansri, N., Kawakami, S., Yokoyama, M., Yamamoto, T., Charoensit, P., Hashida, M., 2008. Anti-tumor effect of all-trans retinoic acid loaded polymeric micelles in solid tumor bearing mice. Pharm. Res. 25, 428–434.

Formelli, F., Clerici, M., Campa, T., Di Mauro, M.G., Magni, A., Mascotti, G., Moglia, D., De Palo, G., Costa, A., Veronesi, U., 1993. Five-year administration of fenretinide: pharmacokinetics and effects on plasma retinol concentrations. J. Clin. Oncol. 11, 2036–2042.

Formelli, F., Barua, A.B., Olson, J.A., 1996. Bioactivities of *N*-(4-hydroxyphenyl) retinamide and retinoyl beta-glucuronide. FASEB J. 10, 1014–1024.

Gaucher, G., Dufresne, M.H., Sant, V.P., Kang, N., Maysinger, D., Leroux, J.C., 2005. Block copolymer micelles: preparation, characterization and application in drug delivery. J. Control Release 109, 169–188.

Hashizume, H., Baluk, P., Morikawa, S., McLean, J.W., Thurston, G., Roberge, S., Jain, R.K., McDonald, D.M., 2000. Openings between defective endothelial cells explain tumor vessel leakiness. Am. J. Pathol. 156, 1363–1380.

Hultin, T.A., May, C.M., Moon, R.C., 1986. *N*-(4-Hydroxyphenyl)-all-trans-retinamide pharmacokinetics in female rats and mice. Drug Metab. Dispos. 14, 714–717.

Kalemkerian, G.P., Slusher, R., Ramalingam, S., Gadgeel, S., Mabry, M., 1995. Growth inhibition and induction of apoptosis by fenretinide in small-cell lung cancer cell lines. J. Natl. Cancer Inst. 87, 1674–1680.

Kataoka, K., Matsumoto, T., Yokoyama, M., Okano, T., Sakurai, Y., Fukushima, S., Okamoto, K., Kwon, G.S., 2000. Doxorubicin-loaded poly(ethylene glycol)–poly(beta-benzyl-L-aspartate) copolymer micelles: their pharmaceutical characteristics and biological significance. J. Control Release 64, 143–153.

Kataoka, K., Harada, A., Nagasaki, Y., 2001. Block copolymer micelles for drug delivery: design, characterization and biological significance. Adv. Drug Deliv. Rev. 47, 113–131.

Kawakami, S., Opanasopit, P., Yokoyama, M., Chansri, N., Yamamoto, T., Okano, T., Yamashita, F., Hashida, M., 2005. Biodistribution characteristics of all-trans retinoic acid incorporated in liposomes and polymeric micelles following intravenous administration. J. Pharm. Sci. 94, 2606–2615.

Kokate, A., Li, X., Jasti, B., 2006. Transport of a novel anti-cancer agent, fenretinide across Caco-2 monolayers. Invest. New Drugs 25, 197–203.

Matsumura, Y., Maeda, H., 1986. A new concept for macromolecular therapeutics in cancer chemotherapy: mechanism of tumoritropic accumulation of proteins and the antitumor agent smancs. Cancer Res. 46, 6387–6392.

Nishiyama, N., Okazaki, S., Cabral, H., Miyamoto, M., Kato, Y., Sugiyama, Y., Nishio, K., Matsumura, Y., Kataoka, K., 2003. Novel cisplatin-incorporated polymeric micelles can eradicate solid tumors in mice. Cancer Res. 63, 8977–8983.

Oku, N., Namba, Y., 1994. Long-circulating liposomes. Crit. Rev. Ther. Drug Carrier Syst. 11, 231–270.

Raffaghello, L., Pagnan, G., Pastorino, F., Cosimo, E., Brignole, C., Marimpietri, D., Montaldo, P.G., Gambini, C., Allen, T.M., Bogenmann, E., Ponzoni, M., 2003. In vitro and in vivo antitumor activity of liposomal Fenretinide targeted to human neuroblastoma. Int. J. Cancer 104, 559–567.

Shabbits, J.A., Chiu, G.N., Mayer, L.D., 2002. Development of an in vitro drug release assay that accurately predicts in vivo drug retention for liposome-based delivery systems. J. Control Release 84, 161–170.

Swanson, B.N., Zaharevitz, D.W., Sporn, M.B., 1980. Pharmacokinetics of *N*-(4-hydroxyphenyl)-all-trans-retinamide in rats. Drug Metab. Dispos. 8, 168–172.

Takahashi, N., Tamagawa, K., Shimizu, K., Fukui, T., Maitani, Y., 2003. Effects on M5076-hepatic metastasis of retinoic acid and *N*-(4-hydroxyphenyl) retinamide, fenretinide entrapped in SG-liposomes. Biol. Pharm. Bull. 26, 1060–1063.

Takakura, Y., Hashida, M., 1996. Macromolecular carrier systems for targeted drug delivery: pharmacokinetic considerations on biodistribution. Pharm. Res. 6, 820–831.

Takino, T., Nakajima, C., Takakura, Y., Sezaki, H., Hashida, M., 1993. Controlled biodistribution of highly lipophilic drugs with various parenteral formulations. J. Drug Target 1, 117–124.

Torchilin, V.P., 2005. Recent advances with liposomes as pharmaceutical carriers. Nat. Rev. Drug Discov. 4, 145–160.

Watanabe, M., Kawano, K., Yokoyama, M., Opanasopit, P., Okano, T., Maitani, Y., 2006. Preparation of camptothecin-loaded polymeric micelles and evaluation of their incorporation and circulation stability. Int. J. Pharm. 308, 183–189.

Yokoyama, M., Opanasopit, P., Okano, T., Kawano, K., Maitani, Y., 2004. Polymer design and incorporation methods for polymeric micelle carrier system containing water-insoluble anti-cancer agent camptothecin. J. Drug Target 12, 373–384.

Yuan, F., Dellian, M., Fukumura, D., Leunig, M., Berk, D.A., Torchilin, V.P., Jain, R.K., 1995. Vascular permeability in a human tumor xenograft: molecular size dependence and cutoff size. Cancer Res. 55, 3752–3756.

Please cite this article in press as: Okuda, T., et al., Block copolymer design for stable encapsulation of *N*-(4-hydroxyphenyl)retinamide into polymeric micelles in mice, Int J Pharm (2008), doi:10.1016/j.ijpharm.2008.01.044

Contents lists available at ScienceDirect

Colloids and Surfaces B: Biointerfaces

journal homepage: www.elsevier.com/locate/colsurfb

A simple hemostasis model for the quantitative evaluation of hydrogel-based local hemostatic biomaterials on tissue surface

Yoshihiko Murakami[a,*], Masayuki Yokoyama[b,**], Hiroshi Nishida[c], Yasuko Tomizawa[c], Hiromi Kurosawa[c]

[a] Department of Organic and Polymer Materials Chemistry, Faculty of Engineering, Tokyo University of Agriculture and Technology, Tokyo 184-8588, Japan
[b] Yokoyama Nano-Medical Polymers Project, Kanagawa Academy of Science and Technology (KAST), Kanagawa, Japan
[c] Department of Cardiovascular Surgery, The Heart Institute of Japan, Tokyo Women's Medical University, Tokyo, Japan

ARTICLE INFO

Article history:
Received 18 March 2008
Received in revised form 30 March 2008
Accepted 7 April 2008
Available online 18 April 2008

Keywords:
Hemostatic hydrogel
Surgical sealant
Quantitative evaluation
Tissue surface
Biointerface

ABSTRACT

Several hemostat hydrogels are clinically used, and some other agents are studied for safer, more facile, and more efficient hemostasis. In the present paper, we proposed a novel method to evaluate local hemostat hydrogel on tissue surface. The procedure consisted of the following steps: (step 1) a mouse was fixed on a cork board, and its abdomen was incised; (step 2) serous fluid was carefully removed because it affected the estimation of the weight gained by the filter paper, and parafilm and preweighted filter paper were placed beneath the liver (parafilm prevented the filter paper's absorption of gradually oozing serous fluid); (step 3) the cork board was tilted and maintained at an angle of about 45° so that the bleeding would more easily flow from the liver toward the filter paper; and (step 4) the bleeding lasted for 3 min. In this step, a hemostat was applied to the liver wound immediately after the liver was pricked with a needle. We found that (1) a careful removal of serous fluid prior to a bleeding and (2) a quantitative determination of the amount of excess aqueous solution that oozed out from a hemostat were important to a rigorous evaluation of hemostat efficacy. We successfully evaluated the efficacy of a fibrin-based hemostat hydrogel by using our method. The method proposed in the present study enabled the quantitative, accurate, and easy evaluation of the efficacy of local hemostatic hydrogel which acts as tissue-adhesive agent on biointerfaces.

1. Introduction

Local hemostatic hydrogels are applied to surgical wounds in order to arrest bleeding from both suture holes and cross-sectional surfaces of parenchymatous organs in cases wherein the use of cautery, ligature, or other conventional hemostatic methods is impractical. The local hemostatic agents include fibrin glue, gelatin-sponge/powder, collagen-sponge/powder/fiber/sheet, oxidized cellulose, and collagen- or gelatin-based hemostatic agents [1]. Moreover, tissue adhesives (such as (1) gelatin with resorcin and formalin, (2) albumin with glutaraldehyde, (3) cyanoacrylate, and (4) synthetic polymers) used for stopping serous fluid and air leaks are also studied for hemostasis [2,3]. Fibrin glues have been widely used in a variety of surgical procedures and are designed to mimic the physiology of the final steps of the blood coagulation cascade. However, there is a risk of infectious contaminations. Collagen and gelatin have high tensile strength, absorbability in the body, and good cell compatibility. They are, however, not suitable as tissue-contacting materials owing to the same risk factor (infectious contaminations). Since synthetic glues do not possess the risk of infectious contaminations, the glues have been actively developed in recent years. For example, cyanoacrylate polymer is comparable to fibrin glues, but it offers additional benefits such as a relatively high bonding strength and no risk of infectious contaminations.

It is important to establish an easy method for the quantitative determination of the efficacy of local hemostatic agents. Various methods have been proposed for the evaluation of hemostat efficacy. For example, Chvapil et al. established a method by which they could arrest moderate bleeding from an anesthetized dog's spleen (bleeding that was induced with a 0.5-cm deep and 4 cm-wide wedge excision) [4]. By means of this method, it was clarified that a hemostatic agent with a sheet-like structure and a hemostatic agent with collagen could stop the bleeding within 3 min, whereas gelatin-sponge or oxidized cellulose materials were less effective. Prior et al. proposed a method wherein estimates of total bleeding

* Corresponding author. Tel.: +81 42 388 7387; fax: +81 42 388 7387.
** Corresponding author. Tel.: +81 44 819 2093; fax: +81 44 819 2095.
E-mail addresses: [illegible] (Y. Murakami),
[illegible] (M. Yokoyama).

0927-7765/$ – see front matter © 2008 Elsevier B.V. All rights reserved.
doi: [illegible]

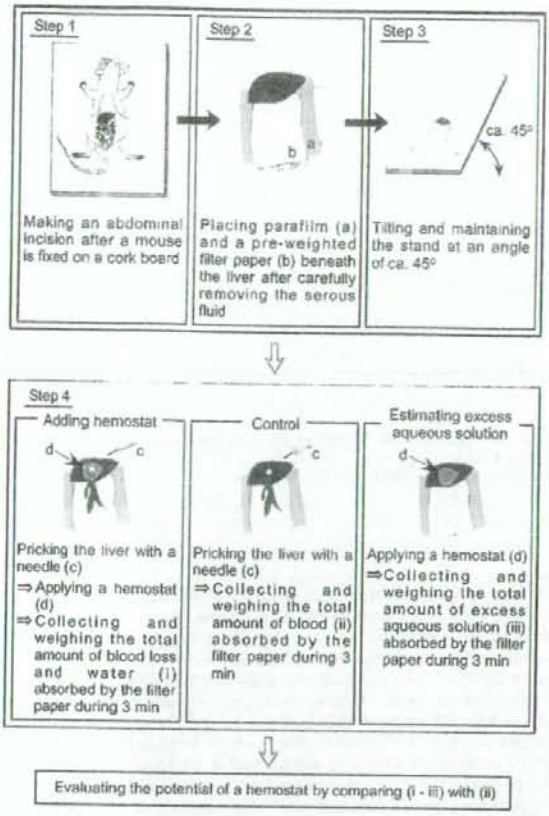

Fig. 1. The proposed method, based on a mouse-hemostasis model, for the quantitative evaluation of local-hemostat hydrogel efficacy on tissue surface.

derived from the weight gained by the preweighted gauze squares or cotton swabs was used to absorb uncoagulated blood from the surgical field of a rabbit kidney [5].

None of these methods are, however, satisfactory for the quantitative determination of the efficacy of local hemostatic agents, because they (1) do not simulate the actual situation where local hemostatic agents are clinically used (i.e., although the rapid completion of a local hemostasis is critical to surgery, some reports neglect how important it is to reduce the formation time of hemostats) or (2) do not present quantitative evaluations, or (3) necessitates complicated procedures. In the present paper, we proposed a novel method to evaluate the efficacy of local hemostat hydrogel on tissue surface.

2. Materials and methods

Fig. 1 illustrates the procedure of the proposed method. The method consists of the following steps: (step 1) a mouse is fixed on a surgical cork board and an abdominal incision was made; (step 2) serous fluid is carefully removed because it affects the estimation of the weight gained by the filter paper, and parafilm and filter paper preweighted by a balance are placed beneath the liver (parafilm prevents the filter paper's absorption of gradually oozing serous fluid); (step 3) the cork board is tilted and maintained at an angle of about 45° to assist the flow of the bleeding from the liver toward the filter paper; and (step 4) the bleeding lasts for 3 min. In this step, a hemostatic agent that is to be evaluated is applied to the liver wound immediately after the liver is pricked with a needle. Also, we performed control experiments (wherein a hemostat is not applied after the liver is pricked with a needle). The operator was blinded so that he did not know whether or not a hemostat was applied in each run (a blind test). The sterile needle (18G, 38 mm, Terumo Corp., Japan) was used for the pricking of the liver. Control experiments were also done, in which we applied a hemostat to the unpricked liver in order to measure the amount of the excess aqueous solution that the filter paper absorbed. This experiment was important because the excess solution oozed out from the hemostat hydrogel during its formation. If this excess solution is not carefully determined and subtracted from the total amount of weight gained in the filter paper, the measured blood would be unjustly higher than the actual amount of blood through bleeding. We determined both the amount of the blood loss and the aqueous solutions after removing the hemostat hydrogel from the filter paper. Cases in which excessive bleeding (blood from the liver reached to the filter paper beneath the liver within 2 s) was seen due to ripping of the liver rather than pricking of the liver were excluded from the evaluation.

We used a fibrin-based hemostat Tisseel™ hydrogel (Baxter, IL) to assess the proposed method. We used 15 ddY mice to evaluate the hemostatic potential of Tisseel, and three ddY mice to estimate the amount of excess solution that oozed out during the hemostat formation. The average weight of the mice was 24.3 g (S.D. 0.61 g). Prior to an abdominal incision, the mice received an intraperitoneal injection of pentobarbital sodium (Nembutal™, Dainippon Pharmaceutical Co. Ltd., Japan). We mixed an aprotinin solution containing fibrinogen and a calcium chloride solution containing thrombin to form a hemostat gel with a dual-chamber applicator. All experiments are performed at room temperature. We performed a statistical analysis of the data by using the two-sided Student's *t*-test. A *P*-value < 0.05 indicated statistical significance.

All animal experiments were carried out according to the Principle of Laboratory Animal Care, the Guide for the Care and Use of Laboratory Animals, and guidelines of the animal care committee in our institute (Tokyo Women's Medical University).

3. Results and discussion

Hydrogel-based adhesives are used for tissue adhesion, hemostasis, and sealing of the leakage of air and body fluids during surgical procedures. The quantitative determination of the efficacy of local hemostatic agents is difficult, because they do not simulate the actual situation where local hemostatic agents are clinically used, do not present quantitative evaluations, and necessitates complicated procedures. In the present paper, we tried to propose a novel method to evaluate local hemostat hydrogel on tissue surface. The procedure consisted of the following easy steps: (1) the fixing of a mouse; (2) the careful removal of serous fluid; (3) the tilting of the cork board at an angle of about 45°; and (4) the bleeding test. The method proposed in the present article can be applied to any surgical site. However, liver was used as a surgical site in a novel mouse model because liver was easy to be exposed.

Fig. 2 shows typical photographs for the Tisseel applications. Tisseel consists of a two-component fibrin matrix that offers highly concentrated human fibrinogen to seal tissue and stop diffuse bleeding. The mixture of the Tisseel gel and the coagulated blood formed after Tisseel was applied to the wound, and consequently, a bleeding was arrested. Tisseel has been used as an adjunct to hemostasis in surgeries involving cardiopulmonary bypass and treatment of splenic injuries due to blunt or penetrating trauma to the abdomen, when control of bleeding by conventional surgical

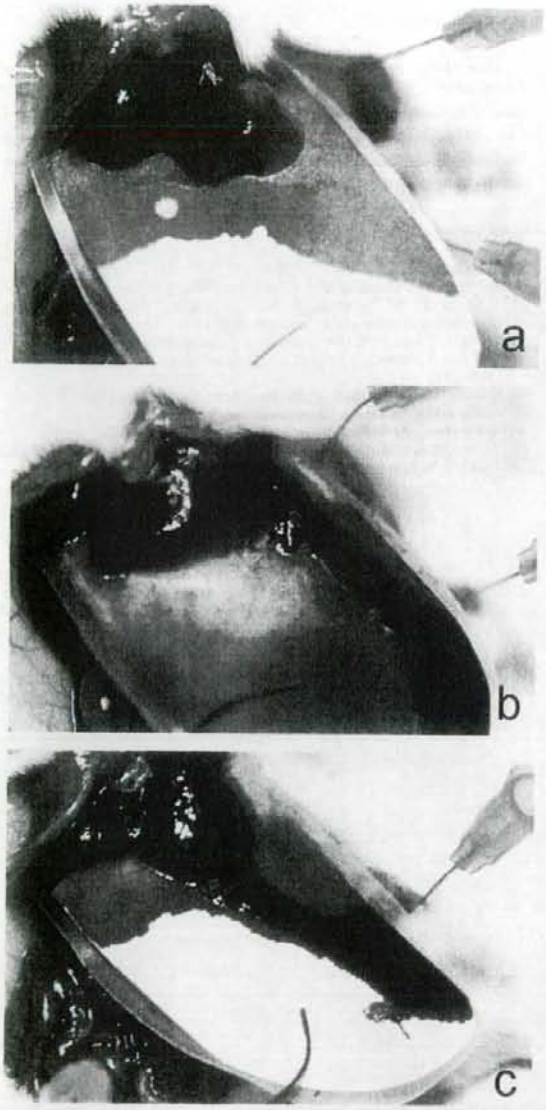

Fig. 2. The typical photographs of Tisseel applications (a: entry 9; b: entry 7; c: entry 8).

techniques, including suture, ligature and cautery, is ineffective or impractical.

Two phenomena were observed in the Tisseel applications. First, the mixture weakly adhered to the tissue surface and arrested the liver hemorrhage (Fig. 2(a)) and second, the mixture did not adhere to the tissue surface and moved slightly owing to bloodstream's force (Fig. 2(b)). The difference between these two phenomena presumably depended on the difference between the rate at which the gel formed and the rate at which the Tisseel gel adhered to the tissue surface. If the gel formation occurred before the gel adhesion, the gel could not successfully anchor to the tissue's uneven surface, resulting in poor tissue adhesiveness. The two phenomena show that Tisseel has poor tissue adhesiveness in such a case as that shown in Fig. 2(b). This observation is the same as that previously

Table 1
Evaluation of the amount of bleeding with (+) or without (−) Tisseel applications (in entries 7 and 8, two filter papers were used)

Entry	Tisseel	Filter paper (mg)	Filter paper + blood (mg)	Blood (mg)
1	+	104	226	122
2		107	222	115
3	+	107	283	176
4	+	104	313	209
5		103	201	98
6		106	219	113
7	+	106	395	311 (289+22)
		100	122	
8		105	382	395 (277+118)
		101	219	
9	+	103	205	102
10		107	178	71
11	+	101	248	147
12		103	299	196
13	+	105	276	171
14	+	103	311	208
15		104	147	43

reported for another fibrin-based glue, BOLHEAL™ [6], where the poly(L-glutamic acid)-based glue exhibited good adhesiveness to tissues where BOLHEAL readily detached. The easy detachment was also clinically observable. In contrast, bleeding was not arrested in the control experiment (Fig. 2(c)).

We found that careful removal of serous fluid prior to bleeding and quantification of the amount of excess aqueous solution that oozed out from a hemostat were important to a rigorous quantitative evaluation of hemostats efficacy. Table 1 summarizes results of the Tisseel applications. The bleeding from the mouse liver was affected by a number of factors such as blood pressure of the mouse and size of the mouse liver. Since these factors were difficult to be controlled in animal experiments, we consider that the difference in bleeding (which is listed in Table 1) was within experimental error. We used 15 mice to minimize the effect of the experimental error.

The average bleeding was 145.9 mg (S.D. 115.6 mg, $N=7$) in the control experiments, whereas it was 180.8 mg (S.D. 64.8 mg, $N=8$) when Tisseel was applied to the wound ($P=0.50$). Although Tisseel exhibited a hemostatic potential, the P-value was unexpectedly high; this was because the amount of excess solution was not considered in the evaluation. The excess solution oozed out from Tisseel after the two precursor solutions were mixed with each other. The average amount of excess solution was 137.0 mg (S.D. 38.5 mg, $N=3$). After a subtraction of the excess solution amount, the reevaluated average bleeding was only 43.8 mg (S.D. 64.8 mg, $N=7$) in mice to whose wounds Tisseel was applied. This value showed that Tisseel had a relatively significant hemostatic potential ($P=0.07$). The difference between the two P values (0.50 and 0.07) showed how important it is to consider the excess solution for the hemostasis evaluations. It is noteworthy that the subtraction of the excess-solution amount from the total measured bleeding has not been considered in previously reported animal hemostasis models [4,5].

Thus, we concluded that the method proposed in the present study facilitated a quantitative, accurate, and easy evaluation of the efficacy of local hemostat hydrogels on tissue surface.

4. Conclusions

Several hemostat hydrogels have been studied for safer, more facile, and more efficient hemostasis. In the present paper, we proposed a novel method to evaluate local hemostat hydrogel on tissue surface. We found that (1) a careful removal of